

# Asymmetric Multiple Description Lattice Vector Quantizers

Suhas N. Diggavi, *Member, IEEE*, N. J. A. Sloane, *Fellow, IEEE*, and Vinay A. Vaishampayan, *Member, IEEE*

**Abstract**—We consider the design of asymmetric multiple description lattice quantizers that cover the entire spectrum of the distortion profile, ranging from symmetric or balanced to successively refinable. We present a solution to a labeling problem, which is an important part of the construction, along with a general design procedure. The high-rate asymptotic performance of the quantizer is also studied. We evaluate the rate-distortion performance of the quantizer and compare it to known information-theoretic bounds. The high-rate asymptotic analysis is compared to the performance of the quantizer.

**Index Terms**—Cubic lattice, high-rate quantization, lattice quantization, multiple descriptions, quantization, source coding, successive refinement, vector quantization.

## I. INTRODUCTION

A MULTIPLE description source encoder generates a set of binary streams or descriptions of a source sequence, each with its own rate constraint. The transmission medium may deliver some or all of the descriptions to the decoder. The objective is to minimize the distortion between the source sequence and the decoded sequence when all the descriptions are available, while ensuring that the distortion which results when only a subset of the descriptions are available remains below a pre-specified value that depends on the subset. If there are  $D$  descriptions, the *distortion profile* is a vector of length  $2^D$  whose components give the distortion constraints for each subset of the descriptions.

In recent years, multiple description coders have received considerable attention, driven by the interest in packet voice and video communications (see the bibliography). Most of the work (with the exception of [11]) has centered around the successively refinable case and the balanced/symmetric case, which are in a sense two extremes of the distortion profile. Successive refinement coders find application in networks with a priority structure whereas balanced codes are useful in networks that do not have such a structure, the best example at the present time being the Internet.

In this paper, we propose a structured scheme that bridges the two cases, in the sense that it permits a fairly general distortion profile to be specified. By allowing the individual descriptions to have different distortions, the quantizer behavior can range

from the balanced case (where each description is equally important) to a strict hierarchy (where the loss of some descriptions could make decoding impossible). The new design is described in terms of a lattice vector quantizer, but the general principle of asymmetric multiple description coding can be extended to many other quantizers, such as trellis-coded quantizers, unstructured vector quantizers, etc. This could potentially allow us to incorporate channel (or network route) reliability information into the transmission. Also, it might be a useful way to allow for less intrinsic wastage of network traffic as some descriptions could be given to the decoder without necessarily waiting for the more important descriptions to arrive (as in successive refinement).

For previous work on the information-theoretic aspects of the multiple description problem see [9], [10], [22], [29], [30]. The problem of designing quantizers for the multiple description problem has been considered in [11], [17], [19], [25], [26], [28]. The work presented in [28] considered only the balanced/symmetric lattice quantizer design. Unlike the work in [11], we do not use a training approach; instead, we use the geometry of the underlying lattice to solve a labeling problem. Other approaches to multiple description coding based on overcomplete expansions are presented in [1], [2], [13] and methods based on optimizing transforms and predictors are presented in [16], [21], [27].

The paper is organized as follows. The source coding problem is formulated in Section II, the design method is described in Section III, properties of the lattices and sublattices needed for the construction are developed in Section IV, a high-rate analysis is presented in Section V, and numerical results are presented in Section VI.

## II. PRELIMINARIES

A block diagram of a two-channel multiple description vector quantizer (MDVQ) using a lattice codebook is shown in Fig. 1. An  $L$ -dimensional source vector  $x$  is first encoded as the closest vector  $\lambda$  in a lattice  $\Lambda \subset \mathbb{R}^L$ . We will write  $\lambda = Q(x)$ . Information about the selected code vector  $\lambda$  is then sent across the two channels, subject to rate constraints imposed by the individual channels. This is done through a labeling function  $\alpha$ . At the decoder, if only channel 1 works, the received information is used to select a vector  $\lambda'_1$  from the channel 1 codebook. If only channel 2 works, the information received over channel 2 is used to select a code vector  $\lambda'_2$  from the channel 2 codebook. If both channels work, it is assumed that enough information is available to recover  $\lambda$ .

Manuscript received December 29, 2000; revised July 5, 2001. The material in this paper was presented in part at the Data Compression Conference (DCC), Snowbird, UT, March 2000.

The authors are with AT&T Shannon Laboratories, Florham Park, NJ 07932 USA (e-mail: suhas@research.att.com; njas@research.att.com; vinay@research.att.com).

Communicated by P. A. Chou, Associate Editor for Source Coding.

Publisher Item Identifier S 0018-9448(02)00007-X.

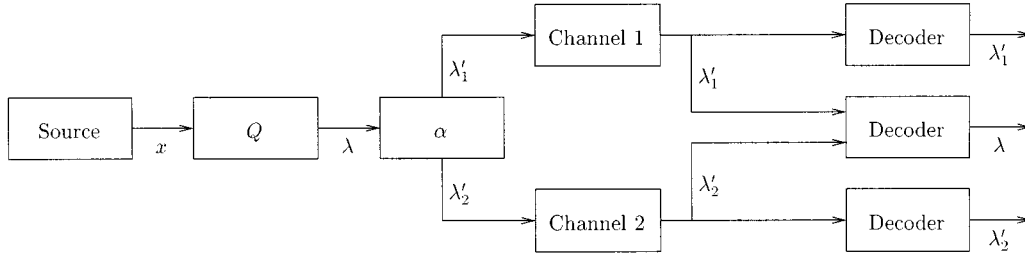


Fig. 1. Block diagram of an MDVQ.

We will assume that the channel 1 and channel 2 codebooks, denoted by  $\Lambda_1$  and  $\Lambda_2$ , respectively, are sublattices<sup>1</sup> of  $\Lambda$ . The index  $[\Lambda : \Lambda_i]$  is denoted by  $N_i$ ,  $i = 1, 2$ .  $N_i$  is also called the *reuse index* of sublattice  $\Lambda_i$ . We assume that each  $\Lambda_i$  is *geometrically similar* to  $\Lambda$ , i.e., that  $\Lambda_i$  can be obtained from  $\Lambda$  by applying a *similarity* (a rotation, change of scale and possibly a reflection). To simplify the analysis we will usually assume that the  $\Lambda_i$  are *strictly similar* to  $\Lambda$ , i.e., that reflections are not used.

*Property P.1:* Let  $\Lambda$  be an  $L$ -dimensional lattice with generator matrix  $G$  (the rows of  $G$  span  $\Lambda$ ). A sublattice  $\Lambda_1 \subseteq \Lambda$  is geometrically strictly similar to  $\Lambda$  if and only if the following condition holds: there is an invertible  $L \times L$  matrix  $U_1$  with integer entries, a scalar  $c_1$ , and an orthogonal  $L \times L$  matrix  $K_1$  with determinant 1 such that a generator matrix for  $\Lambda_1$  can be written as

$$G_1 = U_1 G = c_1 G K_1. \quad (1)$$

If (1) holds then the index of  $\Lambda_1$  in  $\Lambda$  is equal to

$$\begin{aligned} N_1 &= [\Lambda : \Lambda_1] = \sqrt{\frac{\det \Lambda_1}{\det \Lambda}} = \frac{\det G_1}{\det G} \\ &= \det U_1 = c_1^L. \end{aligned} \quad (2)$$

Furthermore,  $\Lambda_1$  has Gram matrix

$$A_1 = G_1 G_1^{tr} = U_1 G G^{tr} U_1^{tr} = U_1 A U_1^{tr} = c_1^2 A \quad (3)$$

where  $A = G G^{tr}$  is a Gram matrix for  $\Lambda$ .

Even if the similarity is not strict, (1)–(3) still hold but with  $\det K_1 = -1$ . Note that the constant  $c_1 > 1$  represents the scaling between the lattice  $\Lambda$  and  $\Lambda_1$  and thus the index  $N_1 = c_1^L$  represents the scaling between the respective volumes of the fundamental regions of the lattices.

We will also usually assume that the sublattices  $\Lambda_1$  and  $\Lambda_2$  are *clean* [3], that is, no point of  $\Lambda$  lies on the boundary of the Voronoi cells of  $\Lambda_1$  or  $\Lambda_2$ . Our algorithm still applies if this condition is not satisfied, but the book-keeping becomes more complicated.

Finally, we require a sublattice of  $\Lambda_1 \cap \Lambda_2$ ,  $\Lambda_s$  (the *product sublattice*) which is geometrically strictly similar to  $\Lambda$  and has index  $N_s = N_1 N_2$  in  $\Lambda$ . To reduce the complexity of the design we will also sometimes make use of a sublattice  $\Lambda_\cap$  of  $\Lambda_1 \cap \Lambda_2$

<sup>1</sup>Strictly speaking, the codebooks are finite subsets of the sublattices  $\Lambda_1$  and  $\Lambda_2$ , but we will ignore that distinction in this paper.

which has index  $N_\cap = \text{lcm}(N_1, N_2)$  in  $\Lambda$  (such sublattices do not always exist—see Section IV).

Since the information sent over channel 1 is used to identify a code vector  $\lambda_1 \in \Lambda_1$ , and the information over channel 2 is used to identify a code vector  $\lambda_2 \in \Lambda_2$ , we will assume that the labeling function  $\alpha$  is a mapping from  $\Lambda$  into  $\Lambda_1 \times \Lambda_2$  and that  $(\lambda_1, \lambda_2) = \alpha(\lambda)$ . The component mappings are  $\lambda_1 = \alpha_1(\lambda)$  and  $\lambda_2 = \alpha_2(\lambda)$ . In order to recover  $\lambda$  when both channels work, it is necessary that  $\alpha$  be one-to-one. This is accomplished by requiring that the ordered pair  $(\lambda_1, \lambda_2)$  is used only once in any labeling scheme.

Given  $\Lambda$ ,  $\Lambda_1$ ,  $\Lambda_2$ , and  $\alpha$ , there are three distortions and two rates associated with the quantizer. For a given source vector  $x$  mapped to the triple  $(\lambda, \lambda_1, \lambda_2)$ , the *two-channel distortion*  $\bar{d}_0$  is given by  $\|x - \lambda\|^2$ , the side distortions  $\bar{d}_i$  by  $\|x - \lambda_i\|^2$ ,  $i = 1, 2$ , where

$$\|\mathbf{x}\|^2 \stackrel{\text{def}}{=} (1/L) \sum_{i=1}^L x_i^2$$

is the dimension-normalized Euclidean norm. The corresponding average distortions are denoted by  $\bar{d}_0$ ,  $\bar{d}_1$ , and  $\bar{d}_2$ . (We will also refer to  $\bar{d}_0$  as the *central distortion*.) We assume that an entropy coder is used to transmit the labeled vectors at a rate arbitrarily close to the entropy, i.e.,  $R_i = \mathcal{H}(\alpha_i(Q(\mathbf{X}))) / L$ ,  $i = 1, 2$ , where  $\mathcal{H}$  is the binary entropy function. The problem is to design the labeling function  $\alpha$  so as to minimize  $\bar{d}_0$  subject to  $\bar{d}_1 \leq D_1$  and  $\bar{d}_2 \leq D_2$ , for given rates  $(R_1, R_2)$  and distortions  $D_1$  and  $D_2$ .

We will assume that the source is memoryless with probability density function (pdf)  $p$ . The  $L$ -fold pdf will be denoted by  $p_L$  where

$$p_L((x_1, x_2, \dots, x_L)) = \prod_{i=1}^L p(x_i).$$

The differential entropies satisfy the relation  $h(p_L) = Lh(p)$ .

Given a lattice  $\Lambda$ , a sublattice  $\Lambda'$ , and a point  $\lambda' \in \Lambda'$ , we denote by  $V_{\Lambda:\Lambda'}(\lambda')$  the set of all points in  $\Lambda$  that are closer to  $\lambda'$  than to any other point in  $\Lambda'$ . This set is the discrete Voronoi set of  $\lambda'$  in  $\Lambda$ . If  $\Lambda'$  is a clean sublattice of  $\Lambda$  we do not need to worry about ties when calculating  $V_{\Lambda:\Lambda'}(\lambda')$ . The Voronoi cell  $V_\Lambda(\lambda)$  of a point  $\lambda \in \Lambda$  is the set of all points in  $\mathbb{R}^L$  that are at least as close to  $\lambda$  as to any other point of  $\Lambda$ . Also,  $\mathcal{E}(\lambda') = \alpha(V_{\Lambda:\Lambda'}(\lambda'))$ ,  $\lambda' \in \Lambda'$ , will denote the set of all labels of the points in  $V_{\Lambda:\Lambda'}(\lambda')$ .

### A. Distortion Computation

The average two-channel distortion  $\bar{d}_0$  is given by

$$\bar{d}_0 = \sum_{\lambda \in \Lambda} \int_{V_\Lambda(\lambda)} \|x - \lambda\|^2 p_L(x) dx. \quad (4)$$

Since the codebook of the quantizer is a lattice, all the Voronoi sets in the above summation are congruent. Furthermore, upon assuming that each Voronoi cell is small and letting  $\nu$  denote the  $L$ -dimensional volume of a Voronoi cell, we obtain the two-channel distortion

$$\bar{d}_0 = \frac{\int_{V_\Lambda(0)} \|x\|^2 dx}{\nu} = G(\Lambda)\nu^{2/L} \quad (5)$$

where the normalized second moment  $G(\Lambda)$  is defined by [5]

$$G(\Lambda) = \frac{\int_{V_\Lambda(0)} \|x\|^2 dx}{\nu^{1+2/L}}. \quad (6)$$

When only description  $i$  is available, for  $i = 1, 2$ , the distortion is given by

$$\bar{d}_i = \bar{d}_0 + \sum_{\lambda \in \Lambda} \|\lambda - \alpha_i(\lambda)\|^2 P(\lambda) \quad (7)$$

where  $P(\lambda)$  is the probability of lattice point  $\lambda$ , and we have assumed that  $\lambda$  is the *centroid* of its Voronoi cell. This is true for the uniform density. For nonuniform densities, there is an error term which goes to zero with the size of the Voronoi cell [14]. The first term in (7) is the two-channel distortion and the second term is the excess distortion which is incurred when only description  $i$  is available. Note that, for a given  $\Lambda$ , only the excess distortion term is affected by the labeling  $\alpha$ .

At this point, we impose a constraint on the labeling function that allows us to reduce the problem to that of labeling a finite number of points. We assume that the labeling function has the *shift invariance* property that  $\alpha(\lambda + \lambda_s) = \alpha(\lambda) + \lambda_s$ , for all  $\lambda_s \in \Lambda_s$ . This leads to the following simplification:

$$\bar{d}_i = \bar{d}_0 + (1/N_s) \sum_{\lambda \in V_{\Lambda:\Lambda_s}(0)} \|\lambda - \alpha_i(\lambda)\|^2 \quad (8)$$

where we have assumed that  $P(\lambda)$  is approximately constant over a Voronoi cell of the sublattice  $\Lambda_s$ , but may vary from one Voronoi cell to another. The consequence of this structural property is that we focus on the labeling of a set of points in  $V_{\Lambda:\Lambda_s}(0)$  and use shifts of this labeling scheme to generate labels for the entire space.

### B. Rate Computation

Let  $R_0$  bits per sample be the rate required to address the two-channel codebook for a single-channel system.<sup>2</sup> We first derive an expression for  $R_0$  and then determine the rates  $R_1$  and  $R_2$ . We use the fact that each quantizer bin has identical volume  $\nu$  and that  $p_L(x)$  is approximately piecewise-constant over each Voronoi cell of  $\Lambda_1$  and  $\Lambda_2$ . This assumption is valid in the limit as the Voronoi cells become small and is standard in asymptotic quantization theory.

<sup>2</sup>This quantity is useful for evaluating the two-channel distortion as well as for evaluating the rate overhead associated with the multiple description system.

The rate  $R_0 = \mathcal{H}(Q(X))$  is given by

$$\begin{aligned} R_0 &= -(1/L) \sum_{\lambda} \int_{V_\Lambda(\lambda)} p_L(x) dx \log_2 \int_{V_\Lambda(\lambda)} p_L(x) dx \\ &\approx -(1/L) \sum_{\lambda} \int_{V_\Lambda(\lambda)} p_L(x) dx \log_2 p_L(\lambda) \nu \\ &\approx h(p) - (1/L) \log_2(\nu). \end{aligned} \quad (9)$$

It can be shown that the rate for description  $i$  is given by

$$R_i = R_0 - (1/L) \log_2(N_i), \quad i = 1, 2. \quad (10)$$

A single-channel system would have used  $R_0$  bits per sample. Instead, a multiple-description system uses a total of  $R_1 + R_2 = 2R_0 - (1/L) \log_2(N_1 N_2)$  bits per sample, and so the rate overhead is  $R_0 - (1/L) \log_2(N_1 N_2)$ .

### III. CONSTRUCTION OF THE LABELING FUNCTION

Suppose  $\Lambda$  is an  $L$ -dimensional lattice with a pair of geometrically strictly similar, clean sublattices  $\Lambda_1$  and  $\Lambda_2$ , and let  $\Lambda_s$  (the product sublattice) be a geometrically strictly similar, clean sublattice of both  $\Lambda_1$  and  $\Lambda_2$ , with indexes  $[\Lambda : \Lambda_1] = N_1$ ,  $[\Lambda : \Lambda_2] = N_2$ , and  $[\Lambda : \Lambda_s] = N_1 N_2$ .

In order to construct a labeling function we first identify  $\mathcal{E}$ , the subset of points of  $\Lambda_1 \times \Lambda_2$  that will be used to label the points of  $\Lambda$ . Informally, we call the ordered pair  $(\lambda_1, \lambda_2)$  an edge and therefore the labeling function is to associate lattice points with edges. A one-to-one correspondence will be established between  $V_{\Lambda:\Lambda_s}(0)$  and a proper subset of  $\mathcal{E}$  so as to minimize an appropriate objective function, while ensuring that the labeling can be extended uniquely to the entire lattice. To this end, we first start by formulating a cost criterion that will be used in the design.

#### A. Cost Criterion

The multiple description problem may be formulated [9] as a problem of minimizing the central distortion subject to constraints on the side distortion. The associated Lagrangian cost criterion is given by

$$\begin{aligned} J &= \bar{d}_0 + \sum_{i=1}^2 \gamma_i \bar{d}_i \\ &= (\gamma_1 + \gamma_2 + 1) \bar{d}_0 + \sum_{i=1}^2 \gamma_i \sum_{\lambda \in \Lambda} \|\lambda - \alpha_i(\lambda)\|^2 P(\lambda) \\ &= (\gamma_1 + \gamma_2 + 1) \bar{d}_0 + \sum_{\lambda \in \Lambda} P(\lambda) \sum_{i=1}^2 \gamma_i \|\lambda - \alpha_i(\lambda)\|^2 \end{aligned} \quad (11)$$

where  $\gamma_1, \gamma_2$  are Lagrange multipliers.

The central distortion  $\bar{d}_0$  is determined by the lattice  $\Lambda$ . If we assume that  $P(\lambda)$  is approximately constant over the Voronoi cell of  $\Lambda_s$ , we can rewrite the cost criterion in terms of the cost over a Voronoi cell of  $\Lambda_s$ . Then the design problem reduces to finding a labeling scheme  $\alpha(\lambda)$  which minimizes

$$\frac{1}{N_s} \sum_{\lambda \in V_{\Lambda:\Lambda_s}(0)} \left[ \gamma_1 \|\lambda - \alpha_1(\lambda)\|^2 + \gamma_2 \|\lambda - \alpha_2(\lambda)\|^2 \right]. \quad (12)$$

After some algebra, the expression inside the summation can be rewritten as

$$\frac{\gamma_1 \gamma_2}{\gamma_1 + \gamma_2} \|\alpha_2(\lambda) - \alpha_1(\lambda)\|^2 + (\gamma_1 + \gamma_2) \left\| \lambda - \frac{\gamma_1 \alpha_1(\lambda) + \gamma_2 \alpha_2(\lambda)}{\gamma_1 + \gamma_2} \right\|^2. \quad (13)$$

The values of  $\gamma_1$  and  $\gamma_2$  determine the relative values of the two side distortions  $\bar{d}_1$  and  $\bar{d}_2$ .

Therefore, our design principle is (informally) for a given pair  $\gamma_1$  and  $\gamma_2$ , to find a labeling function  $\alpha(\lambda)$  such that the sublattice points  $\alpha_1(\lambda) \in \Lambda_1$ ,  $\alpha_2(\lambda) \in \Lambda_2$  are not very far apart and the lattice point  $\lambda \in \Lambda$  that is being labeled is not very far from the weighted mean (the second term of (13)) of these two sublattice points. This general guiding principle leads to our lattice design. (Note that if we have  $\Lambda_1 = \Lambda_2$  then  $R_1 = R_2$ , although we may still introduce some distortion asymmetry by choosing  $\gamma_1 \neq \gamma_2$ .) We will first describe the basic quantizer design and then illustrate it using the lattice  $\mathbb{Z}^2$ .

### B. Lattice Quantizer

The quantizer construction is based on the following steps.

**Step 1)** We are given an  $L$ -dimensional lattice  $\Lambda$ , rates  $R_1$ ,  $R_2$ , and distortions  $D_1$ ,  $D_2$ . These determine the indexes  $N_1$ ,  $N_2$  using (10), and we attempt to find (strictly similar, clean) sublattices  $\Lambda_1$ ,  $\Lambda_2$  with these indexes, together with a product sublattice  $\Lambda_s$ . We also choose appropriate values for the weights  $\gamma_1$  and  $\gamma_2$ . For example, a successively refinable quantizer corresponds to choosing  $\gamma_1 = 1$ ,  $\gamma_2 = 0$ , and  $N_2 = \infty$ . For the balanced case we take  $\gamma_1 = \gamma_2$ . By appropriately choosing  $N_1$ ,  $N_2$ ,  $\gamma_1$ ,  $\gamma_2$ , one can achieve different levels of asymmetry in rate and distortion.

**Step 2)** We find the discrete Voronoi set<sup>3</sup>  $V_0 \stackrel{\text{def}}{=} V_{\Lambda:\Lambda_s}(0)$  for the sublattice  $\Lambda_s$ . This is the fundamental set of points that we will label. The labeling is then extended to the full lattice using the shift invariance property (see Section II). We also find the sets

$$\mathcal{P}_1 = V_{\Lambda_1:\Lambda_s}(0) = V_0 \cap \Lambda_1 \quad (14)$$

$$\mathcal{P}_2 = V_{\Lambda_2:\Lambda_s}(0) = V_0 \cap \Lambda_2 \quad (15)$$

which are the points of  $\Lambda_1$  and  $\Lambda_2$  belonging to the Voronoi set  $V_0$ .

**Step 3)** We determine the set

$$\mathcal{L}_1(\lambda_1) = \{\lambda_2 \in \Lambda_2: \lambda_2 \in V_0 + \lambda_1\} \quad (16)$$

for all  $\lambda_1 \in \mathcal{P}_1$ . These are the points in the sublattice  $\Lambda_2$  which are in the Voronoi set  $V_0$  of  $\Lambda_s$  when translated to be centered at  $\lambda_1 \in \mathcal{P}_1$ . By using these points we ensure that the edge length  $\|\alpha_2(\lambda) - \alpha_1(\lambda)\|^2$  will be minimized (see Property P.8). We will show that each member of  $\mathcal{L}_1(\lambda_1)$  lies in a different coset with respect to the sublattice shifts in  $\Lambda_s$  (Property P.2). Similarly, we determine the set

$$\mathcal{L}_2(\lambda_2) = \{\lambda_1 \in \Lambda_1: \lambda_1 \in V_0 + \lambda_2\} \quad (17)$$

<sup>3</sup>We usually omit the word “discrete” when referring to this set.

for all  $\lambda_2 \in \mathcal{P}_2$ . The set of edges emanating from  $V_0$  is given by

$$\mathcal{E}_{\text{edges}} = \{(\lambda_1, \lambda_2): \lambda_1 \in \mathcal{P}_1, \lambda_2 \in \mathcal{L}_1(\lambda_1)\} \cup \{(\lambda_1, \lambda_2): \lambda_2 \in \mathcal{P}_2, \lambda_1 \in \mathcal{L}_2(\lambda_2)\}. \quad (18)$$

We find a set of coset representatives  $\mathcal{E}_0$  for the equivalence classes of  $\mathcal{E}_{\text{edges}}$  modulo  $\Lambda_s$ . Property P.6 will establish that we can write  $\mathcal{E}_0$  either as

$$\mathcal{E}_0 = \{(\lambda_1, \lambda_2): \lambda_1 \in \mathcal{P}_1 \text{ and } \lambda_2 \in \mathcal{L}_1(\lambda_1)\} \quad (19)$$

or equally well as

$$\mathcal{E}_0 = \{(\lambda_1, \lambda_2): \lambda_2 \in \mathcal{P}_2 \text{ and } \lambda_1 \in \mathcal{L}_2(\lambda_2)\}. \quad (20)$$

**Step 4)** Matching the edges to the lattice points in the Voronoi set is now a straightforward and easily solved assignment problem (cf. [18]). The objective is to label each point in  $V_0$  with edges that are distinct modulo  $\Lambda_s$ , in order that the shift invariance property be satisfied. To formulate this assignment problem we compute the cost given by (12) for each lattice point and each equivalence class of edges modulo  $\Lambda_s$  (taking the minimum over the edge class). This allows us to construct the set of edges which will later be used to label the points in  $V_{\Lambda:\Lambda_s}$ .

If there exists a sublattice  $\Lambda_\cap$  (as defined in Section II) which is also a geometrically strictly similar, clean sublattice of  $\Lambda_1$  and  $\Lambda_2$ , the computational complexity of the design can be further reduced. For then we need only label the points in  $V_{\Lambda:\Lambda_\cap}(0)$ . We will show that this does not reduce the performance of the quantizer—see Property P.9. In this case, we replace the sets  $\mathcal{P}_1$  and  $\mathcal{P}_2$  by the sets  $\mathcal{P}'_1 = V_{\Lambda_1:\Lambda_\cap}(0)$  and  $\mathcal{P}'_2 = V_{\Lambda_2:\Lambda_\cap}(0)$ . The rest of the procedure is unchanged.

### C. Properties of the Quantizer

In this subsection, we state some of the properties of the construction proposed in Section III-B. We have imposed the following restrictions on the labeling scheme.

**Constraint 1:** The labels satisfy the shift property, i.e.,  $\alpha(\lambda + \lambda_s) = \alpha(\lambda) + \lambda_s$ ,  $\forall \lambda_s \in \Lambda_s$ ,  $\lambda \in \Lambda$ .

**Constraint 2:** The labels for  $V_0$  lie in different cosets of the product sublattice: i.e., if  $(\lambda_1, \lambda_2)$  and  $(\lambda_1, \lambda'_2)$  are valid edges then  $\lambda_2$  and  $\lambda'_2$  are in different cosets with respect to the product sublattice.

*Property P.2:* Each member of  $\mathcal{L}_1(\lambda_1)$  lies in a different coset with respect to the sublattice shifts in  $\Lambda_s$ , and  $|\mathcal{L}_1(\lambda_1)| = N_1$ . Similarly, each member of  $\mathcal{L}_2(\lambda_2)$  lies in a different coset with respect to the sublattice shifts in  $\Lambda_s$ , and  $|\mathcal{L}_2(\lambda_2)| = N_2$ .

*Proof:* Let  $\lambda_2, \lambda'_2 \in \mathcal{L}_1(\lambda_1)$ , and  $\lambda'_2 = \lambda_2 + \lambda_s$  for some  $\lambda_s \in \Lambda_s$ . Then  $\lambda'_2 - \lambda_1 = \lambda_2 - \lambda_1 + \lambda_s$ . Hence  $\lambda_2 - \lambda_1$  and  $\lambda'_2 - \lambda_1$  cannot both lie in  $V_0$ . But since  $\lambda_2, \lambda'_2 \in \mathcal{L}_1(\lambda_1)$ ,  $\lambda_2 - \lambda_1$  and  $\lambda'_2 - \lambda_1$  are in  $V_0$ , a contradiction. Thus, each  $\lambda_2 \in \mathcal{L}_1(\lambda_1)$  is in a different coset with respect to the sublattice shifts in  $\Lambda_s$ . Now  $\{V_0 + \lambda'_1\}_{\lambda'_1 = \lambda_1 + \lambda_s, \lambda_s \in \Lambda_s}$  is a partitioning of the points of  $\Lambda$ , and each of these disjoint sets contains points from different cosets of  $\Lambda_2$  (with respect to shifts in  $\Lambda_s$ ). Since

there are only  $N_1$  different cosets of  $\Lambda_2$ ,  $|\mathcal{L}_1(\lambda_1)| \leq N_1$ . In fact, equality must hold, because the space is tiled by such sets and if there were a  $\lambda'_1$  for which  $|\mathcal{L}_1(\lambda'_1)| < N_1$  then would be a  $\lambda_1$  for which  $|\mathcal{L}_1(\lambda_1)| > N_1$ , which is impossible. An identical proof holds for  $\mathcal{L}_2(\lambda_2)$ .  $\square$

*Property P.3:*  $\mathcal{L}_1(\lambda_1)$  consists of the  $N_1$  points  $\lambda_2 \in \Lambda_2$  closest to  $\lambda_1$  subject to the constraint that each  $\lambda_2$  is in a different coset.

*Proof:* We know that

$$\lambda_2 \in \mathcal{L}_1(\lambda_1) \Leftrightarrow \lambda_2 \in V_0 + \lambda_1 \Leftrightarrow \lambda_2 - \lambda_1 \in V_0.$$

Then

$$\lambda_2 - \lambda_1 \in V_0 \Leftrightarrow \|\lambda_2 - \lambda_1\|^2 \leq \|\lambda_2 - \lambda_1 + \lambda_s\|^2$$

for all  $\lambda_s \in \Lambda_s$ . Thus, for any  $\lambda'_2 = \lambda_2 + \lambda_s$ ,  $\lambda_s \neq 0$  we have  $\|\lambda_2 - \lambda_1\|^2 \leq \|\lambda'_2 - \lambda_1\|^2$ , and the claim follows.  $\square$

*Property P.4:*  $\lambda_2 \in \mathcal{L}_1(\lambda_1) \Leftrightarrow \lambda_1 \in \mathcal{L}_2(\lambda_2)$ .

*Proof:* For clean lattices, if  $x \in V_0$  then  $-x \in V_0$  [5]. Then

$$\begin{aligned} \lambda_2 \in \mathcal{L}_1(\lambda_1) &\Leftrightarrow \lambda_2 \in V_0 + \lambda_1 \Leftrightarrow \lambda_2 - \lambda_1 \in V_0 \\ &\Leftrightarrow \lambda_1 - \lambda_2 \in V_0 \Leftrightarrow \lambda_1 \in V_0 + \lambda_2 \Leftrightarrow \lambda_1 \in \mathcal{L}_2(\lambda_2) \quad \square \end{aligned}$$

*Property P.5:* As lattice points in  $\Lambda$  are labeled, the number of times each point from  $\Lambda_1$  is used is  $N_1$  and the number of times each point from  $\Lambda_2$  is used is  $N_2$ .

*Proof:* Let  $N(\lambda_1)$  denote the number of lattice points labeled by  $\lambda_1 \in \Lambda_1$ . Certainly  $N(\lambda_1) \geq N_1$  since  $\lambda_1$  is used  $N_1$  times when we form the edges  $\{(\lambda_1, \lambda_2) : \lambda_2 \in \mathcal{L}_1(\lambda_1)\}$ . If  $\lambda_1$  is used in more than  $N_1$  labels then there is a valid edge  $(\lambda_1, \lambda_2)$  with  $\lambda_2 \notin \mathcal{L}_1(\lambda_1)$ . But this is impossible by Property P.4. Therefore,  $N(\lambda_1) = N_1$  for all  $\lambda_1 \in \Lambda_1$  and similarly  $N(\lambda_2) = N_2$  for all  $\lambda_2 \in \Lambda_2$ .  $\square$

*Property P.6:* The number of cosets in the edge set  $\mathcal{E}_0$  modulo  $\Lambda_s$  is equal to the number of lattice points in  $V_0$ .

*Proof:* Consider the edge set

$$\mathcal{E}_0 = \{(\lambda_1, \lambda_2) : \lambda_1 \in \mathcal{P}_1, \lambda_2 \in \mathcal{L}_1(\lambda_1)\}.$$

From Property P.2, each  $\lambda_2 \in \mathcal{L}_1(\lambda_1)$  lies in a different coset modulo  $\Lambda_s$  and hence each edge  $(\lambda_1, \lambda_2) \in \mathcal{E}_0^{(1)}$  lies in a different coset. As  $|\mathcal{E}_0^{(1)}| = N_1 N_2$ , there are at least that many cosets in the edge set.  $\square$

*Property P.7:* The labeling scheme produces a unique label for each lattice point.

*Proof:* This is immediate from the fact that the labels for the cosets of  $\Lambda/\Lambda_s$  are taken from distinct cosets of  $\mathcal{E}_0/\Lambda_s$ .  $\square$

*Property P.8:* The labeling scheme minimizes the cost criterion given in (11) subject to the coset restriction.

*Proof:* This is an immediate consequence of Property P.3.  $\square$

*Property P.9:* Suppose  $N_1$  and  $N_2$  are not relatively prime, and there exists a sublattice  $\Lambda_\Gamma$  with index  $\text{lcm}\{N_1, N_2\}$  in  $\Lambda$  which is a geometrically strictly similar, clean lattice of  $\Lambda_1$  and  $\Lambda_2$ , and contains  $\Lambda_s$ . Then, we may construct the labeling

to be invariant under shifts by  $\Lambda_\Gamma$ , and obtain the same edge set as if we used the product lattice  $\Lambda_s$ . With this procedure it is necessary to label only  $\text{lcm}\{N_1, N_2\}$  lattice points rather than  $N_1 N_2$  points.

*Proof:* If such a  $\Lambda_\Gamma$  exists then we just need to show that the edge set constructed by using the algorithm with  $\Lambda_s$  can be produced by sublattice shifts of the edge set constructed using  $\Lambda_\Gamma$ . As we saw in the proof of Property P.6, the coset representatives for the edge set are constructed by using

$$\mathcal{E}_0 = \{(\lambda_1, \lambda_2) : \lambda_1 \in \mathcal{P}_1, \lambda_2 \in \mathcal{L}_1(\lambda_1)\}$$

where

$$\mathcal{P}_1 = \bigcup_{\lambda_\Gamma \in \Lambda_\Gamma} \bigcup_{\lambda_1 \in \mathcal{P}'_1} (\lambda_1 + \lambda_\Gamma).$$

Therefore  $\mathcal{E}_0 = \bigcup_{\lambda_\Gamma \in \Lambda_\Gamma} \mathcal{E}'_0$ , where

$$\mathcal{E}'_0 = \{(\lambda_1, \lambda_2) : \lambda_1 \in \mathcal{P}'_1, \lambda_2 \in \mathcal{L}_1(\lambda_1)\}$$

where  $\mathcal{P}'_1 = V_{\Lambda_1 : \Lambda_\Gamma}(0)$ . It follows that there are exactly  $\text{lcm}\{N_1, N_2\}$  coset leader edges in  $\mathcal{E}_0$  with respect to the sublattice  $\Lambda_\Gamma$  and they are given in  $\mathcal{E}'_0$ . Therefore, by matching the cosets of the edges modulo  $\Lambda_\Gamma$  with the lattice points in the Voronoi set for  $\Lambda_\Gamma$ , using the assignment algorithm (as before), and then shifting by  $\Lambda_\Gamma$  we produce exactly the same labeling as we obtained using  $\Lambda_s$ .  $\square$

Property P.9 illustrates that we can reduce computational complexity in the design of the quantizer by using the shift-invariance property of the design over a smaller set of points without any sacrifice in performance. The following Property P.10 can be used to obtain a finer scale of global asymmetry by mixing configurations with different levels of asymmetry. For example, by equally mixing configurations with complementary distortion ratios, we can create globally symmetric side distortions. We call the weighted average of the lattice points  $\frac{\gamma_1 \lambda_1 + \gamma_2 \lambda_2}{\gamma_1 + \gamma_2}$  *representation points*, as they are chosen to be close to the lattice point that the edge represents. Note that distinct edges may share representation points.

*Property P.10:* If there exist several labeling schemes achieving the same cost we can mix these configurations to achieve different levels of asymmetry. A sufficient condition for this to occur is for the number of unique representation points to be smaller than the number of lattice points in the product lattice  $\Lambda_s$ .

*Proof:* The number of representation points is equal to the number of lattice points in the Voronoi set  $V_0$  (see Property P.6). Therefore, if there are some representation points which overlap (i.e., the number of unique representation points is less than the number of points in  $V_0$ ), then there is more than one labeling scheme that produces the same Lagrangian  $\gamma_1 \bar{d}_1 + \gamma_2 \bar{d}_2$ , with each labeling producing different  $\bar{d}_1, \bar{d}_2$ . Suppose one extremal configuration produces the lowest  $\bar{d}_1^{\min}$  and (therefore) the largest  $\bar{d}_2^{\max}$ , and another extremal configuration produces the highest  $\bar{d}_1^{\max}$  and the lowest  $\bar{d}_2^{\min}$ . Then, by using the first configuration in proportion  $\alpha$  and the second in proportion  $\bar{\alpha} = 1 - \alpha$ , one can produce side distortions  $\bar{d}_1 = \alpha \bar{d}_1^{\min} + \bar{\alpha} \bar{d}_1^{\max}$  and  $\bar{d}_2 = \alpha \bar{d}_2^{\max} + \bar{\alpha} \bar{d}_2^{\min}$ . Thus, by keeping the Lagrangian

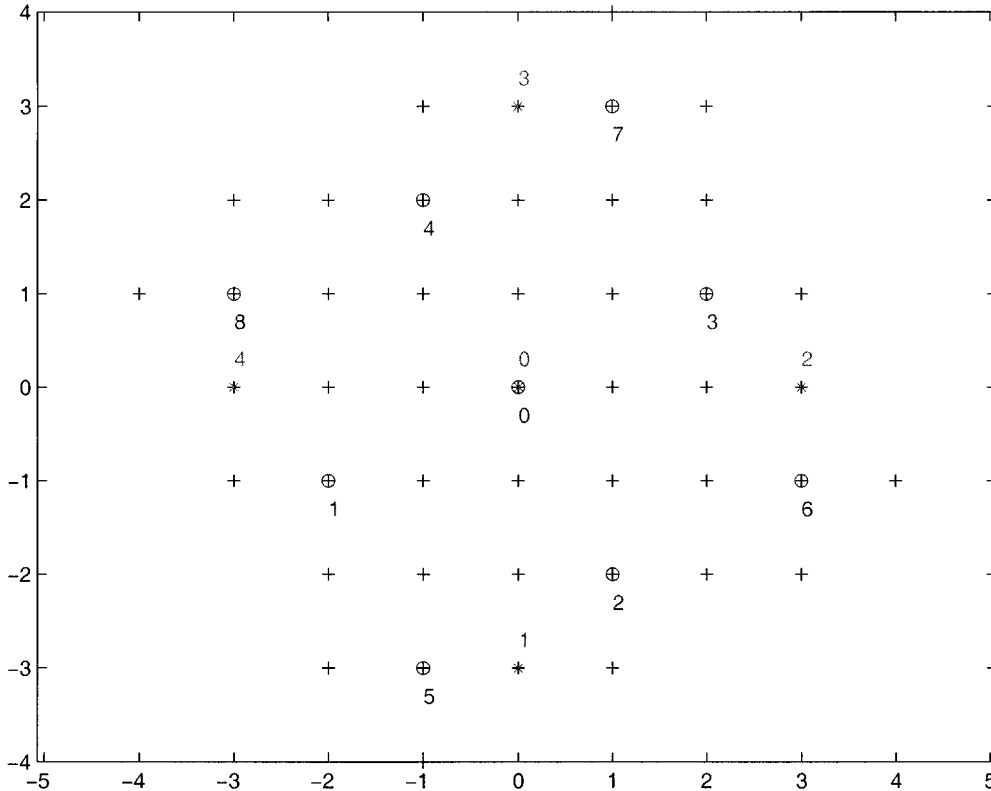


Fig. 2. Elements of  $\Lambda_1$  and  $\Lambda_2$  in Voronoi set  $V_0$  of  $\Lambda_s$ .

cost the same, one can obtain different levels of asymmetry in the distortions  $\bar{d}_1, \bar{d}_2$ .  $\square$

*Remark:* The case of the scalar quantizer ( $L = 1$ ) is of particular interest as these are widely used in practice. For a scalar quantizer,  $\Lambda = \mathbb{Z}$  with  $\Lambda_1 = N_1\mathbb{Z}$ ,  $\Lambda_2 = N_2\mathbb{Z}$ ,  $\Lambda_\cap = \text{lcm}(N_1, N_2)\mathbb{Z}$ , and  $\Lambda_s = N_1N_2\mathbb{Z}$ . The points of  $\lambda_2 \in \Lambda_2$  closest to a point  $\lambda_1 \in \Lambda_1$  are in different cosets with respect to the lattice  $\Lambda_s$ . Therefore, the edge selection procedure outlined in Section III-B is optimal, in that the quantizer design produces the smallest cost as given by (12).

#### D. Example

In this subsection, we illustrate the design procedure with an example in two dimensions using the lattice  $\mathbb{Z}^2$ . We choose  $|\Lambda_1| = 5$  and  $|\Lambda_2| = 9$ . Portions of the two sublattices are shown in Fig. 2 where the points of  $\Lambda_1$  are marked with circles, the points of  $\Lambda_2$  with asterisks, and the points of  $\Lambda_s$  with both circles and asterisks.<sup>4</sup> There are 45 points in the Voronoi set  $V_0$  for  $\Lambda_s$ . The set  $\mathcal{P}_1$  contains nine points of  $\Lambda_1$  and the set  $\mathcal{P}_2$  contains five points of  $\Lambda_2$ . The edges  $\mathcal{E}_{\text{edges}}$  (see (18)) emanating from the points of  $V_0$  are shown in Fig. 3. These are found using the sets  $\mathcal{L}_1(\lambda_1)$  and  $\mathcal{L}_2(\lambda_2)$  for  $\lambda_1 \in \Lambda_1$ ,  $\lambda_2 \in \Lambda_2$ . For example, if we take the point  $\lambda_1 = (2, 1) \in \mathcal{P}_1$ , we see that there are five points in the set  $\mathcal{L}_1(\lambda_1)$ , namely,  $\{(0, 0), (0, 3), (3, 3), (6, 0), (3, 0)\}$ . Note that there are several edges emanating from  $V_0$  which are a sublattice  $\Lambda_s$  shift apart. For example, the edge  $\{(-2, -1), (-6, 0)\}$  is a sublattice  $\Lambda_s$

shift away from the edge  $\{(4, 2), (0, 3)\}$ . To satisfy the shift invariance constraint, we must use only one of these edges to label a point in  $V_0$ . This constraint is built into the optimization procedure. The result of the optimization procedure is illustrated in Fig. 4. Here we have shown only the points in  $\Lambda_0$ . The points in  $\Lambda_1 \cap \Lambda_0$  are marked by circles and those in  $\Lambda_2 \cap \Lambda_0$  by asterisks. Each point carries a pair of labels  $(\lambda_1, \lambda_2)$  with  $\lambda_1 \in \Lambda_1$ ,  $\lambda_2 \in \Lambda_2$ . The complete listing of the labeling is given in Table I. In this example, we have set  $\gamma_1 = 9$  and  $\gamma_2 = 5$ , which determines the respective distortions  $\bar{d}_i$  obtained by the design. A comparison of these distortions with that predicted by information theory is given in Section VI.

## IV. GOOD LATTICES

The lattices that we will investigate and apply in this paper are  $\mathbb{Z}^n$  for  $n = 1, 2$ , or a multiple of 4, together with the root lattices  $D_4$  and  $E_8$  [5]. The analysis could be extended to treat other lattices such as  $\mathbb{Z}^3$ ,  $\mathbb{Z}^6$ , the 12-dimensional Coxeter–Todd lattice, the 16-dimensional Barnes–Wall lattice or the 24-dimensional Leech lattice [5], [20], but we shall not discuss these here.

### A. The Construction of Similar Sublattices

We begin with the observation that multiplication of points in the square lattice  $\mathbb{Z}^2$  (regarded as points in the complex plane) by  $1 + i$  produces a similar sublattice of index 2. All our sublattices will be constructed by generalizing this remark.

We will make use of five types of integers:  $\mathbb{Z}$ , the ordinary *rational integers*;  $\mathcal{G}$ , the ring of *Gaussian integers*  $\{a+bi: a, b \in \mathbb{Z}\}$ ,

<sup>4</sup>In the draft version of this document (see <http://www.research.att.com/~njias/doc/MDVQ.html>, May 2001), the circles are blue and the crosses are red.

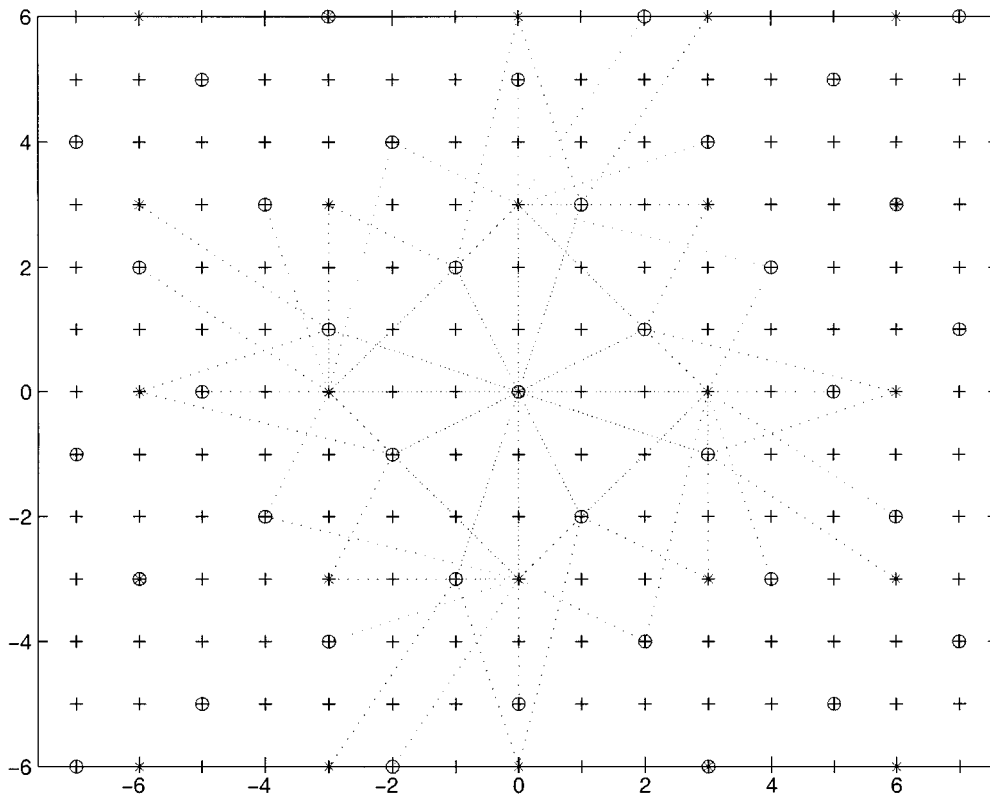


Fig. 3. Edges emanating from the Voronoi cell of the sublattice.

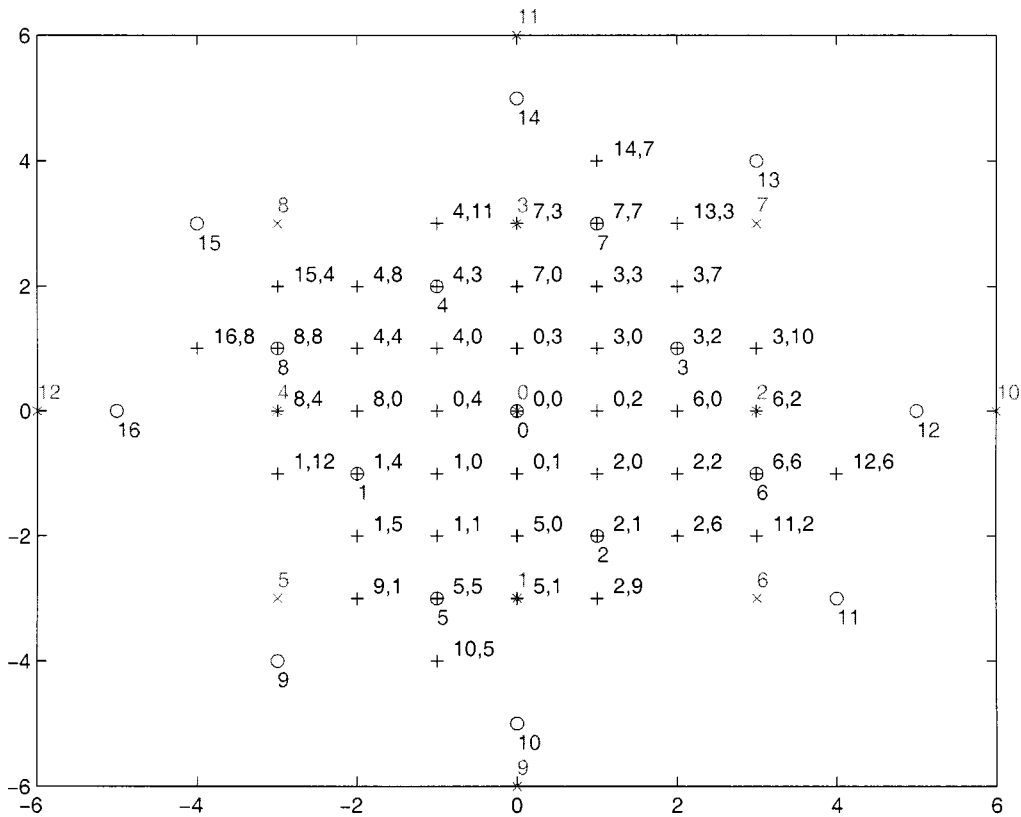


Fig. 4. Labels generated by the algorithm.

where  $i = \sqrt{-1}$ ;  $\mathcal{J}$ , the ring of Eisenstein integers  $\{a + b\omega : a, b \in \mathbb{Z}\}$ , where  $\omega = e^{2\pi i/3}$ ;  $\mathbb{H}_0$ , the ring of Lipschitz integral quaternions  $\{a + bi + cj + dk : a, b, c, d \in \mathbb{Z}\}$ , where  $i, j, k$  are the familiar unit quaternions; and  $\mathbb{H}_1$ , the ring of Hurwitz

TABLE I  
LATTICE POINTS AND LABELS FOR A VORONOI SET OF THE PRODUCT  
SUBLATTICE AS LABELED IN FIG. 4

$\lambda$	$\lambda_1$	$\lambda_2$	$\lambda$	$\lambda_1$	$\lambda_2$	$\lambda$	$\lambda_1$	$\lambda_2$
(0,0)	(0,0)	(0,0)	(-1,0)	(0,0)	(-3,0)	(0,-1)	(0,0)	(0,-3)
(1,0)	(0,0)	(3,0)	(0,1)	(0,0)	(0,3)	(-1,-1)	(-2,-1)	(0,0)
(-1,1)	(-1,2)	(0,0)	(1,-1)	(1,-2)	(0,0)	(1,1)	(2,1)	(0,0)
(-2,0)	(-3,1)	(0,0)	(0,-2)	(-1,-3)	(0,0)	(2,0)	(3,-1)	(0,0)
(0,2)	(1,3)	(0,0)	(-2,1)	(-1,2)	(-3,0)	(1,-2)	(1,-2)	(0,-3)
(-2,-1)	(-2,-1)	(-3,0)	(2,-1)	(1,-2)	(3,0)	(2,1)	(2,1)	(3,0)
(-1,2)	(-1,2)	(0,3)	(-1,-2)	(-2,-1)	(0,-3)	(1,2)	(2,1)	(0,3)
(2,-2)	(1,-2)	(3,-3)	(-2,-2)	(-2,-1)	(-3,-3)	(-2,2)	(-1,2)	(-3,3)
(2,2)	(2,1)	(3,3)	(0,-3)	(-1,-3)	(0,-3)	(3,0)	(3,-1)	(3,0)
(-3,0)	(-3,1)	(-3,0)	(0,3)	(1,3)	(0,3)	(3,-1)	(3,-1)	(3,-3)
(-3,-1)	(-2,-1)	(-6,0)	(1,-3)	(1,-2)	(0,-6)	(-1,-3)	(-1,-3)	(-3,-3)
(-3,1)	(-3,1)	(-3,3)	(-1,3)	(-1,2)	(0,6)	(3,1)	(2,1)	(6,0)
(1,3)	(1,3)	(3,3)	(-3,2)	(-4,3)	(-3,0)	(3,-2)	(4,-3)	(3,0)
(-2,-3)	(-3,-4)	(0,-3)	(2,3)	(3,4)	(0,3)	(-4,1)	(-5,0)	(-3,3)
(4,-1)	(5,0)	(3,-3)	(-1,-4)	(0,-5)	(-3,-3)	(1,4)	(0,5)	(3,3)

*integral quaternions*  $\{a + bi + cj + dk : a, b, c, d \text{ all in } \mathbb{Z} \text{ or all in } \mathbb{Z} + \frac{1}{2}\}$ . Other rings of integers could also be used, but these suffice for the lattices considered in this paper.

If  $\Lambda = \mathbb{Z}$ , multiplication of lattice points by  $\xi \in \mathbb{Z}$  gives  $\xi\mathbb{Z}$ , a similar sublattice of index  $N = |\xi|$ .

If  $\Lambda = \mathbb{Z}^2 = \mathcal{G}$ , multiplication by the Gaussian integer  $\xi = a + bi \in \mathcal{G}$  gives a similar sublattice  $\Lambda' = \xi\Lambda$  of index  $N = a^2 + b^2$ . A number  $N$  is of the form  $a^2 + b^2$  if and only if it is of the form

$$2^{e_1} \prod_{p_i \equiv 1(4)} p_i^{f_i} \prod_{q_j \equiv 3(4)} q_j^{2g_j} \quad (21)$$

where the first product is over primes  $p_i$  congruent to 1 (mod 4), the second product is over primes  $q_j$  congruent to 3 (mod 4), and  $e_1, f_i$ , and  $g_j$  are nonnegative integers. These indexes are the numbers

$$1, 2, 4, 5, 8, 9, 10, 13, 16, 17, 18, 20, \dots \quad (22)$$

of [24, Sequence A1481].

If  $\Lambda = A_2 = \mathcal{J}$ , the planar hexagonal lattice, multiplication by the Eisenstein integer  $\xi = a + b\omega \in \mathcal{J}$  gives a similar sublattice  $\Lambda' = \xi\Lambda$  of index  $N = a^2 + ab + b^2$ . A number  $N$  is of the form  $a^2 + ab + b^2$  if and only if primes congruent to 2 (mod 3) appear to even powers. These indexes are the numbers

$$1, 3, 4, 7, 9, 12, 13, 16, 19, 21, 25, 27, \dots \quad (23)$$

of [24, Sequence A3136].

It is shown in [3] that the above conditions are also necessary: if  $\mathbb{Z}$ ,  $\mathbb{Z}^2$ , or  $A_2$  has a similar sublattice of index  $N$  then  $N$  must have the form described in the preceding paragraphs.

For the lattices  $\Lambda = \mathbb{Z}^4, \mathbb{Z}^8, \mathbb{Z}^{12}, \dots, D_4$ , and  $E_8$  a necessary condition for the existence of a geometrically similar sublattice of index  $N$  is that  $N$  should be of the form  $m^{L/2}$  for some integer  $m$ , where  $L$  is the dimension. This condition is also sufficient, since such sublattices can be obtained by writing

$m = a^2 + b^2 + c^2 + d^2$ , regarding  $\Lambda$  as a sublattice of  $\mathbb{H}_0^{L/4}$ , and multiplying  $\Lambda$  on the left or on the right by the quaternion  $\xi = a + bi + cj + dk$ . Left and right multiplications in general give different sublattices. In the case of  $D_4$  and  $E_8$ , we may also multiply by Hurwitz integral quaternions to obtain further similar sublattices.

Odd-dimensional lattices of dimension greater than 1 are less interesting. For a lattice  $\Lambda$  of odd dimension  $L$  has a geometrically similar sublattice of index  $N$  if and only if  $N$  is an  $L$ th power, say  $m^L$ , and sublattices of this index can be obtained by scalar multiplication of  $\Lambda$  by  $m$  (see [3]).

The *norm* of a quaternion  $\xi = a + bi + cj + dk$  is  $\xi\bar{\xi} = a^2 + b^2 + c^2 + d^2$  where the bar denotes quaternionic conjugation. If  $\xi$  belongs to one of the above rings, the index of the sublattice  $\xi\Lambda$  (or  $\Lambda\xi$ ) in  $\Lambda$ ,  $[\Lambda : \xi\Lambda]$ , is equal to  $(\xi\bar{\xi})^{L/2}$ , where  $L$  is the dimension and the bar is complex or quaternionic conjugation as appropriate.

## B. Clean Sublattices

In dimension one, the sublattice  $\xi\mathbb{Z}$  is clean if and only if  $\xi$  is odd.

Reference [3] gives necessary and sufficient conditions for a similar sublattice of any two-dimensional lattice to be clean. In particular, the sublattice  $\xi\mathbb{Z}^2$  ( $\xi = a + ib$ ) is clean if and only if  $N = a^2 + b^2$  is odd. These indexes are obtained by setting  $e_1 = 0$  in (21)

$$1, 5, 9, 13, 17, 25, 29, 37, 41, 45, \dots$$

[24, Sequence A57653].

The sublattice  $\xi A_2$  ( $\xi = a + b\omega$ ) is clean if and only if  $a$  and  $b$  are relatively prime. It follows that  $A_2$  has a clean similar sublattice of index  $N$  if and only if  $N$  is a product of primes congruent to 1 (mod 6). These are the numbers

$$1, 7, 13, 19, 31, 37, 43, 49, 61, 67, \dots \quad (24)$$

[24, Sequence A57654].

The existence of clean sublattices in dimensions greater than two was not considered in [3].

We can give a fairly complete answer for the lattices  $\mathbb{Z}^L$ ,  $L \geq 1$ .

*Theorem IV.1:* Suppose  $L \geq 1$  and  $\mathbb{Z}^L$  has a geometrically similar sublattice  $\Lambda'$  of index  $N$ . Then  $\Lambda'$  is clean if and only if  $N$  is odd.

*Proof:* (If) Let  $\Lambda' = \phi(\mathbb{Z}^L)$ , where  $\phi$  is a similarity, and let  $\Lambda'' = \phi^{-1}(\mathbb{Z}^L)$ . If  $\phi$  multiplies lengths by  $c_1$  (as in (1)) then  $N = c_1^L$ . Suppose  $N = c_1^L$  is odd and let  $\Lambda'$  have generator matrix  $K$ , with  $KK^{tr} = c_1^2 I_L = mI_L$ , where  $m = c_1^2$ . (In the notation of (1),  $U_1 = c_1 K_1 = K$ .) Note that as  $KK^{tr}$  has integer entries,  $m = c_1^2$  is an integer and as  $N^2 = m^L$  is odd, so is  $m$ . Since  $\Lambda'$  is a sublattice of  $\mathbb{Z}^L$ , the entries of  $K$  are integers. Then  $\Lambda''$  has generator matrix  $K^{-1} = \frac{1}{m} K^{tr}$ .

We must show that there are no points of  $\mathbb{Z}^L$  on the boundary of the Voronoi cell of  $\Lambda'$ , or, equivalently, that there are no points of  $\Lambda''$  on the boundary of the Voronoi cell of  $\mathbb{Z}^L$ .

It is enough to consider just one face of the Voronoi cell of  $\mathbb{Z}^L$ , say that consisting of the points  $P = (\frac{1}{2}, \frac{x_2}{2}, \frac{x_3}{2}, \dots, \frac{x_L}{2})$ ,

where  $|x_i| \leq 1$  for  $2 \leq i \leq L$ . If  $P \in \Lambda''$  then there is a vector  $u = (u_1, \dots, u_L) \in \mathbb{Z}^L$  such that

$$P = \frac{1}{m} u K^{tr}. \quad (25)$$

Equating the first components we get that

$$\frac{1}{2} = \frac{1}{m} \quad \text{times a vector with integer entries.}$$

Since  $m$  is odd this is impossible.

(Only if) Suppose  $N$  is even, then as  $N^2 = m^L$ ,  $m$  is also an even integer. We claim that all the vertices of the Voronoi cell for  $\mathbb{Z}^L$  (i.e., all the deep holes in  $\mathbb{Z}^L$  in the notation of [5]) belong to  $\Lambda''$ . In fact, (25) implies that  $u = PK$ . Let  $P$  be a vector of the form  $(\pm\frac{1}{2}, \pm\frac{1}{2}, \dots, \pm\frac{1}{2})$ , and let  $K = (k_{ij})$ . From  $KK^{tr} = K^{tr}K = mI_L$  we have  $\sum_{i=1}^L k_{ij}^2 = m$  and, since  $k_{ij}^2 \equiv k_{ij} \pmod{2}$ ,  $\sum_{i=1}^L k_{ij}$  is even (for all  $j$ ). Hence  $PK$  has integer entries and is in  $\mathbb{Z}^L$ .  $\square$

The following corollary summarizes our results about  $\mathbb{Z}^L$  for the values of  $L$  that we are interested in. Note that since  $\mathbb{Z}^L$  has no ‘‘handedness,’’ there is essentially no difference between ‘‘similar’’ and ‘‘strictly similar’’ for this lattice.

*Corollary IV.1:*  $\mathbb{Z}^L$  has a geometrically similar sublattice of index  $N$  if and only if

- $N$  is an  $L$ th power, if  $L$  is odd;
- $N$  is of the form  $a^2 + b^2$ , if  $L = 2$ ;
- $N$  is of the form  $m^{L/2}$  for some integer  $m$ , if  $L = 4k$ ,  $k \geq 1$ .

In each case the sublattice is clean if and only if  $N$  is odd. The same results hold if ‘‘similar’’ is replaced by ‘‘strictly similar.’’

For  $D_4$  we have only a partial answer.

*Theorem IV.2:* If  $M$  is 7 or a product of primes congruent to 1 (mod 4) then  $D_4$  has a geometrically strictly similar, clean sublattice of index  $M^2$ . The values of  $M$  mentioned are

$$1, 5, 7, 13, 17, 25, 29, 37, 41, 53, \dots \quad (26)$$

(7 together with [24, Sequence A4613].

*Proof:* We take our standard version of the  $D_4$  lattice to have minimal norm 2 (as in [5]) and generator matrix

$$G = \begin{bmatrix} 1 & 1 & 0 & 0 \\ -1 & 0 & 1 & 0 \\ 0 & -1 & 0 & 1 \\ 0 & -1 & 0 & -1 \end{bmatrix}. \quad (27)$$

The four rows  $v_1, v_2, v_3, v_4$  of  $G$  correspond to the nodes of the Coxeter diagram for  $D_4$  shown in Fig. 5, where  $v_i \cdot v_i = 2$  ( $i = 1, \dots, 4$ ), two nodes that are joined by an edge correspond to vectors with inner product  $-1$ , and two nodes that are not joined by an edge are orthogonal.

We regard  $D_4$  as a subset of

$$\mathcal{H} = \{w + xi + yj + zk : w, x, y, z \in \mathbb{R}\}$$

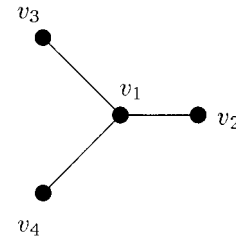


Fig. 5. Coxeter diagram for any lattice that is geometrically similar to  $D_4$ : there are four generating vectors  $v_1, v_2, v_3, v_4$  satisfying  $v_1 \cdot v_1 = v_2 \cdot v_2 = v_3 \cdot v_3 = v_4 \cdot v_4$ ,  $v_i \cdot v_j = -\frac{1}{2} v_1 \cdot v_1$  if nodes  $v_i$  and  $v_j$  are joined by an edge, and  $v_i \cdot v_j = 0$  ( $i \neq j$ ) otherwise.

the space of real quaternions. Our sublattices  $\Lambda'$  will be constructed by multiplying  $D_4$  either on the left or on the right by appropriate Hurwitzian integral quaternions. If

$$\xi = a + bi + cj + dk \in \mathcal{H}$$

then  $\xi D_4$  has generator matrix  $GL_\xi$ , where

$$L_\xi = \begin{bmatrix} a & b & c & d \\ -b & a & d & -c \\ -c & -d & a & b \\ -d & c & -b & a \end{bmatrix} \quad (28)$$

and  $D_4 \xi$  has generator matrix  $GR_\xi$ , where

$$R_\xi = \begin{bmatrix} a & b & c & d \\ -b & a & -d & c \\ -c & d & a & -b \\ -d & -c & b & a \end{bmatrix}. \quad (29)$$

Note that

$$L_\xi L_\xi^{tr} = R_\xi R_\xi^{tr} = mI_4, \quad L_\xi R_\xi = R_\xi L_\xi \quad (30)$$

where  $m = \xi \bar{\xi} = a^2 + b^2 + c^2 + d^2$ .

We will show that under certain conditions,  $D_4$  and  $D_4 \xi$  are clean sublattices. We only give the proof for  $D_4 \xi$ , the other case being completely analogous.

The Voronoi cell for  $D_4$  is a 24-cell, with 24 octahedral faces [4], [5]. A typical face (they are all equivalent) is that lying in the hyperplane

$$X \cdot v_1 = \frac{1}{2} v_1 \cdot v_1 \quad (31)$$

having center  $\delta_0 = \frac{1}{2} v_1$  and six vertices

$$\begin{aligned} \delta_1 &= \frac{1}{2} (2v_1 + v_3 + v_4) \\ \delta_2 &= \frac{1}{2} (-v_3 - v_4) \\ \delta_3 &= \frac{1}{2} (2v_1 + v_2 + v_3) \\ \delta_4 &= \frac{1}{2} (-v_2 - v_3) \\ \delta_5 &= \frac{1}{2} (2v_1 + v_2 + v_4) \\ \delta_6 &= \frac{1}{2} (-v_2 - v_4) \end{aligned} \quad (32)$$

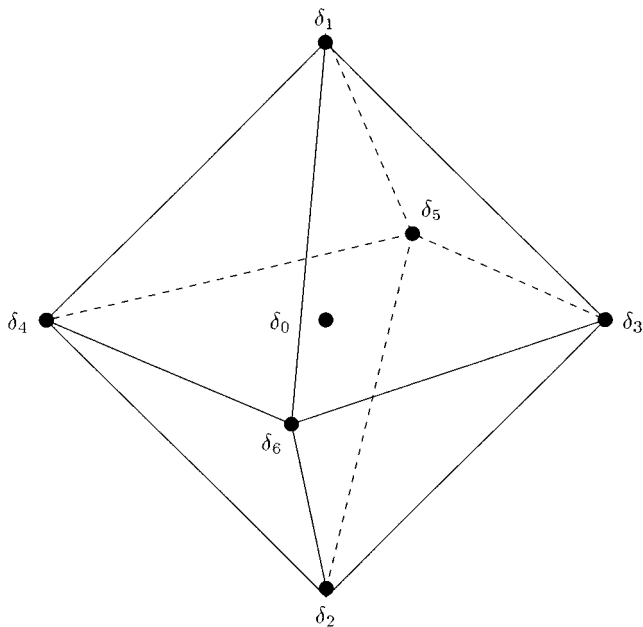


Fig. 6. Labeling for center and vertices of octahedral face of Voronoi cell for  $D_4$ .

(see Fig. 6). A point  $X$  belongs to this face if and only if it satisfies (31) and

$$|(X - \delta_0) \cdot (\delta_1 - \delta_0)| + |(X - \delta_0) \cdot (\delta_3 - \delta_0)| + |(X - \delta_0) \cdot (\delta_5 - \delta_0)| \leq \frac{1}{4} v_1 \cdot v_1. \quad (33)$$

Let  $\Lambda' = D_4 \xi$ , where  $\xi$  is a quaternion of the form

$$\xi = \frac{\alpha}{2} + \frac{\alpha}{2} i + \frac{\beta}{2} j + \frac{\beta}{2} k \quad (34)$$

and  $\alpha$  and  $\beta$  are odd, positive, relatively prime integers. The norm of  $\xi$  is  $\frac{1}{2}(\alpha^2 + \beta^2)$ . Then we claim that  $\Lambda'$  is clean.

To show this, we begin by computing the generator matrix for  $\Lambda'$  as follows:

$$G' = GR_\xi = \begin{bmatrix} 0 & \alpha & 0 & \beta \\ \frac{-\alpha-\beta}{2} & \frac{-\alpha+\beta}{2} & \frac{\alpha-\beta}{2} & \frac{-\alpha-\beta}{2} \\ \frac{\alpha-\beta}{2} & \frac{-\alpha-\beta}{2} & \frac{\alpha+\beta}{2} & \frac{\alpha-\beta}{2} \\ \frac{\alpha+\beta}{2} & \frac{-\alpha+\beta}{2} & \frac{-\alpha+\beta}{2} & \frac{-\alpha-\beta}{2} \end{bmatrix} \quad (35)$$

and denote its rows by  $v'_1, v'_2, v'_3, v'_4$ . We will similarly use primes to denote the center ( $\delta'_0$ ) and vertices ( $\delta'_1, \dots, \delta'_6$ ) of an octahedral face of the Voronoi cell of  $\Lambda'$ . From (32) we find that

$$\begin{aligned} \delta'_0 &= \frac{1}{2} (0, \alpha, 0, \beta) \\ \delta'_1 &= \frac{1}{2} (\alpha, \alpha, \beta, \beta) \\ \delta'_3 &= \frac{1}{2} (-\beta, \alpha, \alpha, \beta) \\ \delta'_5 &= \frac{1}{2} (0, \alpha + \beta, 0, -\alpha + \beta). \end{aligned}$$

We must show that it is impossible for a point

$$X = (w, x, y, z) \in D_4$$

to satisfy the primed versions of (31) and (33), which are

$$\alpha x + \beta z = \frac{1}{2}(\alpha^2 + \beta^2) \quad (36)$$

$$|\alpha w + \beta y| + |-\beta w + \alpha y| + |\beta x - \alpha z| \leq \frac{1}{2}(\alpha^2 + \beta^2). \quad (37)$$

Suppose, on the contrary, that  $(w, x, y, z) \in D_4$  satisfies (36) and (37). From (36) we have

$$z = \frac{1}{2\beta}(\alpha^2 + \beta^2 - 2\alpha x) \quad (38)$$

and from (37)

$$|\beta x - \alpha z| \leq \frac{1}{2}(\alpha^2 + \beta^2)$$

which together imply

$$\frac{1}{2}(\alpha - \beta) \leq x \leq \frac{1}{2}(\alpha + \beta).$$

So we may write  $x = \frac{1}{2}(\alpha + \mu)$ , say, where  $\mu$  is an odd integer satisfying  $-\beta \leq \mu \leq \beta$ , and from (38)

$$z = \frac{\beta^2 - \alpha\mu}{2\beta}$$

which implies  $\alpha\mu \equiv \beta^2 \pmod{2\beta}$ . Since  $\beta$  is odd,  $\beta^2 \equiv \beta \pmod{2\beta}$ , and we conclude that

$$\alpha\mu \equiv \beta \pmod{2\beta}. \quad (39)$$

Thus, for some integer  $k$ ,  $\alpha\mu - \beta = 2k\beta$  and since  $\alpha$  and  $\beta$  are relatively prime,  $\beta$  must divide  $\mu$ . Therefore  $\mu = \pm\beta$ . But this is impossible. For if  $\mu = \beta$ ,  $x = \frac{1}{2}(\alpha + \beta)$ ,  $z = \frac{1}{2}(-\alpha + \beta)$ ,  $\beta x - \alpha z = \frac{1}{2}(\alpha^2 + \beta^2)$ , and then (37) implies  $w = y = 0$ , so  $w + x + y + z = \beta \notin D_4$ , since  $\beta$  is odd. A similar argument applies if  $\mu = -\beta$ .

So far we have shown that if  $\alpha$  and  $\beta$  are odd, positive, and relatively prime, then the sublattice  $D_4 \xi$  is clean, where  $\xi$  is given by (34). Suppose  $M$  is a product of primes congruent to  $1 \pmod{4}$ . From the classical theory of quadratic forms (see, for example, [6]), we know that  $M = p^2 + q^2$  with  $p$  even,  $q$  odd, and  $\gcd(p, q) = 1$ . We now simply set  $\alpha = p + q$  and  $\beta = |p - q|$ .

It remains to discuss the case  $M = 7$ . For this we can multiply on the left or on the right by either of the quaternions

$$\xi = \frac{1}{2} + \frac{1}{2}i + \frac{1}{2}j + \frac{5}{2}k \quad \text{or} \quad \frac{1}{2} + \frac{3}{2}i + \frac{3}{2}j + \frac{3}{2}k.$$

We omit the straightforward verification that these sublattices are clean.  $\square$

In the other direction we have the following.

**Theorem IV.3:**  $D_4$  has no clean, geometrically similar sublattice of index  $M^2$  if  $M$  is 3, 9, or 11.

*Proof:* The proof is by exhaustive search, using a computer. We produced a list of all vectors of norm  $2M$  in  $D_4$ , and from this we found all similar sublattices of index  $M^2$  by finding all sets of four vectors corresponding to the Coxeter diagram of Fig. 5. Given a sublattice  $\Lambda'$ , we compute the equations defining an octahedral face of the Voronoi cell from (31) and

(33). Then AMPL [12] and CPLEX [7] were used to verify that in every case there was a point of  $D_4$  on the face.  $\square$

The preceding discussion has shown that the lattices  $\mathbb{Z}$ ,  $\mathbb{Z}^2$ ,  $\mathbb{Z}^{4k}$  for  $k \geq 1$  and  $D_4$  have a plentiful supply of clean, geometrically similar sublattices. We expect the same will be true of the  $E_8$  lattice, but this question is presently under investigation.

Finally, we remark that if  $\Lambda'$  is a clean sublattice of  $\Lambda$  and  $\Lambda''$  is a clean sublattice of  $\Lambda'$ , then  $\Lambda''$  is a clean sublattice of  $\Lambda$ .

### C. Common Sublattices of $\Lambda_1$ and $\Lambda_2$

We begin with a general comment. Let  $\Lambda_1$  and  $\Lambda_2$  be any two sublattices of a lattice  $\Lambda$  (they must have the same dimension as  $\Lambda$  but are otherwise arbitrary). Then we may form their intersection  $\Lambda_\cap = \Lambda_1 \cap \Lambda_2$  and their join  $\Lambda_\cup = \Lambda_1 \cup \Lambda_2$ , as shown in Fig. 7. The join is the lattice generated by the vectors of both  $\Lambda_1$  and  $\Lambda_2$  (and, in general, is not simply their union). From the Second Isomorphism Theorem of group theory (e.g., [23]) the indexes and determinants of these lattices are related by

$$[\Lambda_\cup : \Lambda_1] = [\Lambda_2 : \Lambda_\cap], \quad [\Lambda_\cup : \Lambda_2] = [\Lambda_1 : \Lambda_\cap] \quad (40)$$

$$\det \Lambda_1 \det \Lambda_2 = \det \Lambda_\cup \det \Lambda_\cap. \quad (41)$$

There are now in general many ways to find a “product” sublattice  $\Lambda_s \subset \Lambda_\cap$  with

$$[\Lambda : \Lambda_s] = [\Lambda : \Lambda_1][\Lambda : \Lambda_2]. \quad (42)$$

Let  $\Lambda$  be one of  $\mathbb{Z}$ ,  $\mathbb{Z}^2$ , or  $A_2$ , and let  $\Lambda_1 = \xi_1 \Lambda$ ,  $\Lambda_2 = \xi_2 \Lambda$  be geometrically strictly similar sublattices obtained by multiplying  $\Lambda$  by elements of  $\mathbb{Z}$ ,  $\mathcal{G}$ , or  $\mathcal{J}$ , respectively. Since these three rings are unique factorization rings, the notions of greatest common divisor (gcd) and least common multiple (lcm) are well-defined. We set  $\xi_\cup = \gcd(\xi_1, \xi_2)$ ,  $\xi_\cap = \text{lcm}\{\xi_1, \xi_2\}$ , and then it is easy to see that  $\Lambda_\cup = \xi_\cup \Lambda$ ,  $\Lambda_\cap = \xi_\cap \Lambda$ . We can also form the product sublattice  $\Lambda_s = \xi_1 \xi_2 \Lambda$  (see Fig. 8). The indexes of these lattices are given by

$$\begin{aligned} [\Lambda : \Lambda_1] &= (\xi_1 \bar{\xi}_1)^{L/2}, & [\Lambda : \Lambda_2] &= (\xi_2 \bar{\xi}_2)^{L/2} \\ [\Lambda : \Lambda_\cup] &= (\xi_\cup \bar{\xi}_\cup)^{L/2}, & [\Lambda : \Lambda_\cap] &= (\xi_\cap \bar{\xi}_\cap)^{L/2} \\ [\Lambda : \Lambda_s] &= [\Lambda : \Lambda_1][\Lambda : \Lambda_2]. \end{aligned} \quad (43)$$

In dimension  $L = 1$ , (43) implies that

$$[\Lambda : \Lambda_\cap] = \text{lcm}\{[\Lambda : \Lambda_1], [\Lambda : \Lambda_2]\} \quad (44)$$

and we can take  $\Lambda_{\text{lcm}} = \Lambda_\cap$ . However, if  $L = 2$ , (44) does not hold in general.

In dimensions one or two, if  $\xi_1$  and  $\xi_2$  are relatively prime (meaning  $\gcd(\xi_1, \xi_2) = 1$ ), we have  $\xi_\cup = 1$ ,  $\xi_\cap = \xi_1 \xi_2$ ,  $\Lambda = \Lambda_\cup$ ,  $\Lambda_s = \Lambda_\cap$ .

Because the quaternions form a noncommutative ring their arithmetic theory is more complicated. For example, it is necessary to distinguish between left gcd's and right gcd's. Both are well-defined in  $\mathbb{H}_1$  and also in  $\mathbb{H}_0$  as long as at least one of the quaternions involved has odd norm [8], [15]. We plan to discuss this theory and its applications to the study of sublattices of  $\mathbb{Z}^4$  and  $D_4$  elsewhere. In the present paper, we will restrict our attention to a narrow class of sublattices, which, however, will be

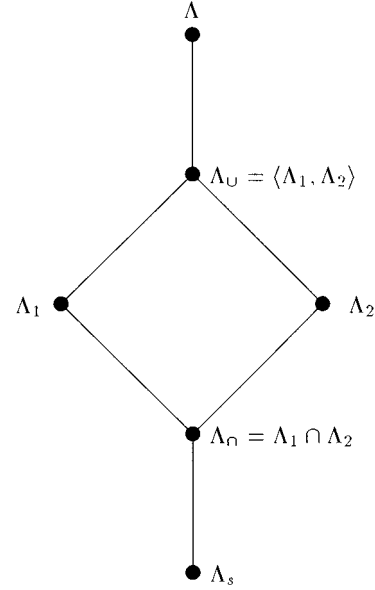


Fig. 7. Intersection, join, and “product” sublattice of two arbitrary sublattices.

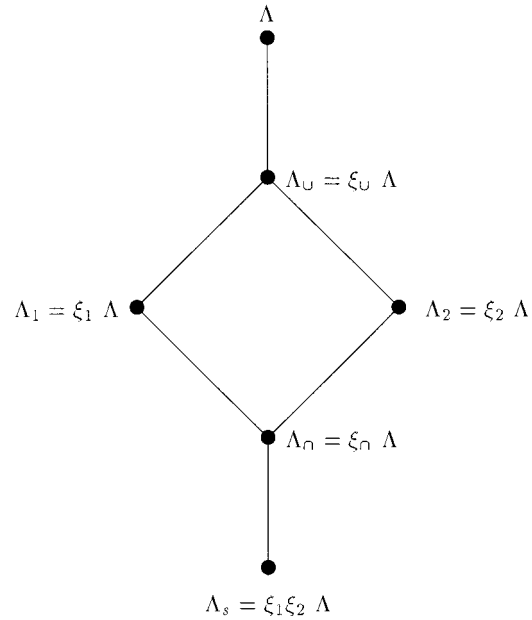


Fig. 8. Join  $\Lambda_\cup$ , intersection  $\Lambda_\cap$ , and product  $\Lambda_s$  of two sublattices  $\Lambda_1, \Lambda_2$  of  $\Lambda$ , where  $\Lambda$  is one of  $\mathbb{Z}$ ,  $\mathbb{Z}^2$ , or  $A_2$ .

general enough to provide an adequate supply of sublattices for our applications.

For  $\mathbb{Z}^4$ , we choose two Lipschitz integral quaternions  $\xi_1, \xi_2 \in \mathbb{H}_0$  whose norms are odd and relatively prime. For  $D_4$  we choose two Hurwitz integral quaternions

$$\begin{aligned} \xi_1 &= \frac{1}{2} \alpha_1 (1 + i) + \frac{1}{2} \beta_1 (j + k) \in \mathbb{H}_1 \\ \xi_2 &= \frac{1}{2} \alpha_2 (1 + i) + \frac{1}{2} \beta_2 (j + k) \in \mathbb{H}_1 \end{aligned} \quad (45)$$

where  $\alpha_1, \alpha_2, \beta_1, \beta_2$  are odd positive integers with

$$\begin{aligned} \gcd(\alpha_1, \beta_1) &= \gcd(\alpha_2, \beta_2) \\ &= \gcd((\alpha_1^2 + \beta_1^2)/2, (\alpha_2^2 + \beta_2^2)/2) = 1. \end{aligned}$$

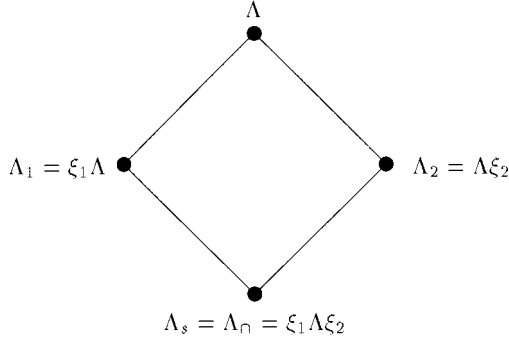


Fig. 9.  $\Lambda_1$  (resp.,  $\Lambda_2$ ) obtained by multiplying  $\Lambda = \mathbb{Z}^4$  or  $D_4$  on the left (resp., right) by a quaternion  $\xi_1$  (resp.,  $\xi_2$ ).

In both cases, we take  $\Lambda_1 = \xi_1 \Lambda$ ,  $\Lambda_2 = \Lambda \xi_2$ , and  $\Lambda_s = \Lambda_r = \xi_1 \Lambda \xi_2$  (see Fig. 9). Then

$$\begin{aligned} [\Lambda : \Lambda_1] &= (\xi_1 \bar{\xi}_1)^2, & [\Lambda : \Lambda_2] &= (\xi_2 \bar{\xi}_2)^2 \\ [\Lambda : \Lambda_s] &= [\Lambda : \Lambda_1][\Lambda : \Lambda_2]. \end{aligned} \quad (46)$$

For  $\mathbb{Z}^4$  this gives sublattices  $\Lambda_1, \Lambda_2$  of indexes  $M_1^2, M_2^2$ , where  $M_1$  and  $M_2$  are any two relatively prime odd numbers (from Corollary IV.1). For  $D_4$ ,  $M_1$  and  $M_2$  are any two relatively prime numbers from (26).

## V. HIGH-RATE ASYMPTOTICS

In this section we analyze the distortion of the asymmetric multiple description lattice quantizer at high rates.

Let  $\bar{\Lambda}$  be an  $L$ -dimensional lattice with geometrically strictly similar, clean sublattices  $\bar{\Lambda}_1, \bar{\Lambda}_2, \bar{\Lambda}_r = \bar{\Lambda}_1 \cap \bar{\Lambda}_2, \bar{\Lambda}_s$  (as in Fig. 7), with indexes  $\bar{N}_1, \bar{N}_2, \bar{N}_r$  and  $\bar{N}_s$ , respectively, where  $\bar{N}_s = \bar{N}_1 \bar{N}_2$ . It is assumed that  $\nu_{\bar{\Lambda}}$ , the volume of a fundamental region for  $\bar{\Lambda}$ , is equal to unity. A sequence of lattices is then obtained from the base set of lattices by scaling each component. Let  $\Lambda_1(n) = n\bar{\Lambda}_1$ ,  $\Lambda_2(n) = n\bar{\Lambda}_2$ ,  $\Lambda_r(n) = n\bar{\Lambda}_r$ , and  $\Lambda_s(n) = n^2\bar{\Lambda}_s$ . These have indexes  $N_1(n) = n^L \bar{N}_1$ ,  $N_2(n) = n^L \bar{N}_2$  with  $N_r(n) = n^L \bar{N}_r$ ,  $N_s(n) = n^{2L} \bar{N}_s$  where  $N_s(n) = N_1(n)N_2(n)$ . As the index of the lattices grows, we scale the lattices by a factor  $\beta$  so that the overall rate also grows (see (59)).

We analyze the rate-distortion performance for the set of lattices  $\{\Lambda, \Lambda_1(n), \Lambda_2(n), \Lambda_r(n), \Lambda_s(n)\}$ . However, in order to keep the notation simple, we will only use the sequence index  $n$  when it is necessary to avoid confusion. Thus, we will write  $\Lambda_s$  instead of  $\Lambda_s(n)$ ,  $N_s$  instead of  $N_s(n)$ , and so on.

Referring to (11), let

$$J_s = \sum_{\lambda \in \Lambda} P(\lambda) \sum_i \gamma_i \|\lambda - \alpha_i(\lambda)\|^2. \quad (47)$$

We investigate the high-rate behavior of  $J_s$  and then find the approximation for  $\bar{d}_i$ ,  $i = 1, 2$ . The latter would also allow us to predict the asymmetry in the distortion behavior of the quantizer. The reader is referred to Fig. 10 for the analysis. Note that in the figure we have written  $\bar{\gamma}_i = \frac{\gamma_i}{\gamma_1 + \gamma_2}$  for brevity.

Let

$$J_{s_1} = \sum_{\lambda \in \Lambda} \frac{\gamma_1 \gamma_2}{\gamma_1 + \gamma_2} \|\alpha_2(\lambda) - \alpha_1(\lambda)\|^2 P(\lambda) \quad (48)$$

and

$$J_{s_2} = \sum_{\lambda \in \Lambda} (\gamma_1 + \gamma_2) \left\| \lambda - \frac{\gamma_1 \alpha_1(\lambda) + \gamma_2 \alpha_2(\lambda)}{\gamma_1 + \gamma_2} \right\|^2 P(\lambda). \quad (49)$$

Then, using (13)

$$J_s = J_{s_1} + J_{s_2}. \quad (50)$$

Under the assumption that  $\Lambda_r$  is fine enough for  $P(\lambda)$  to be considered a constant over  $V_{\Lambda_r}$  we obtain

$$J_{s_1} = \frac{\gamma_1 \gamma_2}{\gamma_1 + \gamma_2} \sum_{\lambda' \in \Lambda_r} P(\lambda') \sum_{\lambda \in V_{\Lambda_r}(\lambda')} \|\alpha_1(\lambda) - \alpha_2(\lambda)\|^2. \quad (51)$$

By construction, the inner sum in (51) does not depend on  $\lambda'$ . Therefore, taking this out of the outer summation and using  $\sum_{\lambda' \in \Lambda_r} P(\lambda') = 1/N_r$ , we obtain

$$J_{s_1} = \frac{\gamma_1 \gamma_2}{\gamma_1 + \gamma_2} \frac{1}{N_r} \sum_{\lambda \in V_{\Lambda_r}(0)} \|\alpha_1(\lambda) - \alpha_2(\lambda)\|^2 \quad (52)$$

which can be written in terms of the edge endpoints as

$$J_{s_1} = \frac{\gamma_1 \gamma_2}{\gamma_1 + \gamma_2} \frac{1}{N_r} \sum_{\lambda_1 \in V_{\Lambda_r}(0)} \sum_{\lambda_2 \in V_{\Lambda_s}(\lambda_1)} \|\lambda_1 - \lambda_2\|^2. \quad (53)$$

Observe that the edges in (52) are not the same as those in (53), since the points  $\lambda \in V_{\Lambda_r}(0)$  need not be labeled using  $\lambda_1 \in V_{\Lambda_r}(0)$ . However, in both cases, there is exactly one edge from each coset of  $\mathcal{E}_0/\Lambda_s$ . Since all edges in a coset have equal length, the sums in (52) and (53) are identical.

Using the Riemann approximation

$$\int_{V_{\Lambda_s}(\lambda_1)} \|x - \lambda_1\|^2 dx \approx \sum_{\lambda_2 \in V_{\Lambda_s}(\lambda_1)} \|\lambda_2 - \lambda_1\|^2 \nu_2 \quad (54)$$

for the summation in (53) we obtain

$$J_{s_1} = \frac{\gamma_1 \gamma_2}{\gamma_1 + \gamma_2} \frac{1}{N_r} \sum_{\lambda_1 \in V_{\Lambda_r}(0)} \frac{1}{\nu_2} \left[ \frac{\int_{V_s(\lambda_1)} \|x - \lambda_1\|^2 dx}{\nu_s^{(1+2/L)}} \right] \nu_s^{(1+2/L)} \quad (55)$$

The term within the brackets is  $G(\Lambda_s)$ , the normalized second moment of a Voronoi cell of  $\Lambda_s$  ( $= \frac{1}{12}$  for the square lattice),  $\nu_2 = N_2$ ,  $\nu_s = N_1 N_2$ , and  $N_r/[\Lambda_1 : \Lambda_r] = N_1$ . Therefore,

$$J_{s_1} = \frac{\gamma_1 \gamma_2}{\gamma_1 + \gamma_2} \frac{[\Lambda_1 : \Lambda_r]}{N_r \nu_2} G(\Lambda_s) \nu_s^{1+2/L} \quad (56)$$

$$\stackrel{(a)}{=} \frac{\gamma_1 \gamma_2}{\gamma_1 + \gamma_2} G(\Lambda_s) \nu_s^{2/L} \quad (57)$$

where (a) follows because  $[\Lambda_1 : \Lambda_r] = N_r/N_1$  and  $\nu_s = N_1 N_2$ . If all the lattices in question are scaled by  $\beta$ , then

$$J_{s_1} = \beta^{2L} \frac{\gamma_1 \gamma_2}{\gamma_1 + \gamma_2} G(\Lambda_s) (N_1 N_2)^{2/L}. \quad (58)$$

The rate of the  $i$ th description is given by

$$R_i = h(p) - \frac{1}{L} \log_2(N_i) - \frac{1}{L} \log_2(\beta^L), \quad i = 1, 2. \quad (59)$$

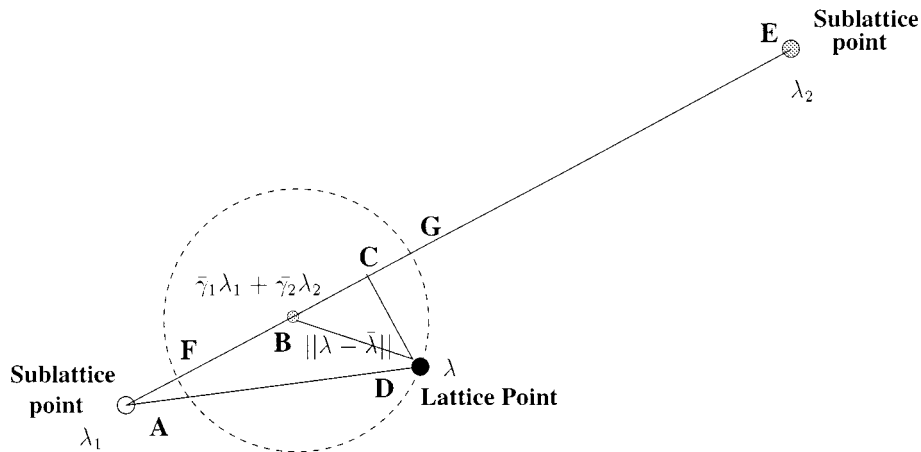


Fig. 10. Relationship of edge length and distortion.

Therefore,

$$N_i = \frac{1}{\beta^L} 2^{Lh(p)} 2^{-LR_i}, \quad i = 1, 2. \quad (60)$$

The scale factor  $\beta^2$  is related to the differential entropy of the source and the rate  $R_0$  through

$$\beta^2 = 2^{2h(p)} 2^{-2R_0}. \quad (61)$$

Using (60) and (61) in (58) we obtain

$$J_{s_1} \approx \frac{\gamma_1 \gamma_2}{\gamma_1 + \gamma_2} G(\Lambda_s) 2^{2h(p)} 2^{-2(R_1 + R_2 - R_0)}. \quad (62)$$

A bound for  $J_{s_2}$  may be obtained in terms of  $\rho_\Gamma$ , the covering radius of  $\Lambda_\Gamma$ , by observing that for every  $\lambda$ , it is possible through a suitable  $\Lambda_\Gamma$  shift to satisfy

$$\left\| \lambda - \frac{\gamma_1 \alpha_1(\lambda) + \gamma_2 \alpha_2(\lambda)}{\gamma_1 + \gamma_2} \right\| \leq \rho_\Gamma. \quad (63)$$

Note that<sup>5</sup>  $\rho_\Gamma = \Theta(n)$  as the volume of  $\Lambda_\Gamma$  is growing as  $n^L$ . Thus, we have the inequality

$$J_{s_2} \leq (\gamma_1 + \gamma_2) \rho_\Gamma^2 \beta^2. \quad (64)$$

By comparing (58) and (64) we observe that  $J_{s_1} = \Theta(n^4 \beta^2)$  whereas  $J_{s_2} = \Theta(n^2 \beta^2)$ . As  $\nu_s = N_1 N_2 = \Theta(n^{2L})$  and  $\rho_\Gamma = \Theta(n)$  we find that  $J_{s_1}$  dominates  $J_{s_2}$  and we obtain the approximation

$$J \approx \frac{\gamma_1 \gamma_2}{\gamma_1 + \gamma_2} G(\Lambda_s) 2^{2h(p)} 2^{-2(R_1 + R_2 - R_0)} \quad (65)$$

where  $R_0$  determines the central distortion  $\bar{d}_0$  and is given by  $\bar{d}_0 = G(\Lambda) 2^{2(h(p) - R_0)}$  (see (5)).

<sup>5</sup>Here the notation  $f(n) = \Theta(g(n))$  denotes that  $f(n) = O(g(n))$  as well as  $g(n) = O(f(n))$ . Here  $f(n) = O(g(n))$  means  $\limsup_{n \rightarrow \infty} \left| \frac{f(n)}{g(n)} \right| < \infty$

### A. Side Distortions

The approximations to the side distortions are obtained by using Fig. 10 and the following analysis. The channel 1 distortion is given by

$$\bar{d}_1 = \frac{1}{N_\Gamma} \sum_{\lambda \in V_{\Lambda_\Gamma}(0)} \|\alpha_1(\lambda) - \lambda\|^2 + \bar{d}_0. \quad (66)$$

Our goal is to examine the behavior of

$$\frac{1}{N_\Gamma} \sum_{\lambda \in V_{\Lambda_\Gamma}(0)} \|\alpha_1(\lambda) - \lambda\|^2$$

at high rates. To this end we write

$$\begin{aligned} \|\lambda_1 - \lambda\|^2 &= \|(\lambda_1 - \bar{\lambda}) + (\bar{\lambda} - \lambda)\|^2 \\ &= \|(\lambda_1 - \bar{\lambda})\|^2 + \|(\bar{\lambda} - \lambda)\|^2 + 2\langle (\lambda_1 - \bar{\lambda}), (\bar{\lambda} - \lambda) \rangle \end{aligned} \quad (67)$$

where  $\bar{\lambda} = (\gamma_1 \lambda_1 + \gamma_2 \lambda_2) / (\gamma_1 + \gamma_2)$ , giving the double inequality

$$\begin{aligned} &\|(\lambda_1 - \bar{\lambda})\|^2 + \|(\bar{\lambda} - \lambda)\|^2 - 2|\langle (\lambda_1 - \bar{\lambda}), (\bar{\lambda} - \lambda) \rangle| \\ &\leq \|\lambda_1 - \lambda\|^2 \leq \|(\lambda_1 - \bar{\lambda})\|^2 + \|(\bar{\lambda} - \lambda)\|^2 \\ &\quad + 2|\langle (\lambda_1 - \bar{\lambda}), (\bar{\lambda} - \lambda) \rangle| \end{aligned} \quad (68)$$

and by use of the Cauchy-Schwartz inequality [18]

$$\begin{aligned} &\|(\lambda_1 - \bar{\lambda})\|^2 + \|(\bar{\lambda} - \lambda)\|^2 - 2\|(\lambda_1 - \bar{\lambda})\| \|(\bar{\lambda} - \lambda)\| \\ &\leq \|\lambda_1 - \lambda\|^2 \leq \|(\lambda_1 - \bar{\lambda})\|^2 + \|(\bar{\lambda} - \lambda)\|^2 \\ &\quad + 2\|(\lambda_1 - \bar{\lambda})\| \|(\bar{\lambda} - \lambda)\|. \end{aligned} \quad (69)$$

This can be rewritten as

$$\begin{aligned} \|\lambda_1 - \bar{\lambda}\|^2 \left[ 1 - \frac{\|\lambda - \bar{\lambda}\|}{\|\lambda_1 - \bar{\lambda}\|} \right]^2 &\leq \|\lambda - \lambda_1\|^2 \\ &\leq \|\lambda_1 - \bar{\lambda}\|^2 \left[ 1 + \frac{\|\lambda - \bar{\lambda}\|}{\|\lambda_1 - \bar{\lambda}\|} \right]^2. \end{aligned} \quad (70)$$

We now justify the geometrical relationship shown in Fig. 10 (note that this only holds at high rates). The main point of the analysis is that the distance  $AD^2 = \|\lambda - \lambda_1\|^2$  is well approximated by  $AB^2 = \|\bar{\lambda} - \lambda_1\|^2$  at high rate. Note that this need not be true on an edge-by-edge basis, but is true in an average sense as formalized below.

Summing (69) over  $\lambda \in V_{\Lambda_\Gamma}(0)$ , and using  $\|\bar{\lambda} - \lambda\|^2 \geq 0$  we obtain

$$\begin{aligned} & \sum_{\lambda \in V_{\Lambda_\Gamma}(0)} \{ \|\lambda_1 - \bar{\lambda}\|^2 - 2\|\lambda_1 - \bar{\lambda}\| \|\bar{\lambda} - \lambda\| \} \\ & \leq \sum_{\lambda \in V_{\Lambda_\Gamma}(0)} \|\lambda - \lambda_1\|^2 \\ & \leq \sum_{\lambda \in V_{\Lambda_\Gamma}(0)} \{ \|\lambda_1 - \bar{\lambda}\|^2 + \|\bar{\lambda} - \lambda\|^2 \\ & \quad + 2\|\lambda_1 - \bar{\lambda}\| \|\bar{\lambda} - \lambda\| \}. \end{aligned} \quad (71)$$

Rewriting the above equation we get

$$\begin{aligned} & \left[ \sum_{\lambda \in V_{\Lambda_\Gamma}(0)} \|\lambda_1 - \bar{\lambda}\|^2 \right] \left[ 1 - 2 \frac{\sum_{\lambda \in V_{\Lambda_\Gamma}(0)} \|\lambda_1 - \bar{\lambda}\| \|\bar{\lambda} - \lambda\|}{\sum_{\lambda \in V_{\Lambda_\Gamma}(0)} \|\lambda_1 - \bar{\lambda}\|^2} \right] \\ & \leq \sum_{\lambda \in V_{\Lambda_\Gamma}(0)} \|\lambda - \lambda_1\|^2 \\ & \leq \left[ \sum_{\lambda \in V_{\Lambda_\Gamma}(0)} \|\lambda_1 - \bar{\lambda}\|^2 \right] \left[ 1 + \frac{\sum_{\lambda \in V_{\Lambda_\Gamma}(0)} \|\bar{\lambda} - \lambda\|^2}{\sum_{\lambda \in V_{\Lambda_\Gamma}(0)} \|\lambda_1 - \bar{\lambda}\|^2} \right. \\ & \quad \left. + 2 \frac{\sum_{\lambda \in V_{\Lambda_\Gamma}(0)} \|\lambda_1 - \bar{\lambda}\| \|\bar{\lambda} - \lambda\|}{\sum_{\lambda \in V_{\Lambda_\Gamma}(0)} \|\lambda_1 - \bar{\lambda}\|^2} \right]. \end{aligned} \quad (72)$$

Using these inequalities and the fact that  $\|\lambda - \bar{\lambda}\| \leq \rho_\Gamma$ , we obtain the following result.

*Lemma V.1:* If  $\gamma_1 \neq 0$ ,  $\gamma_2 \neq 0$

$$\lim_{R_1 \rightarrow \infty} \sum_{\lambda \in V_{\Lambda_\Gamma}(0)} \|\lambda - \lambda_1\|^2 = \lim_{R_1 \rightarrow \infty} \sum_{\lambda \in V_{\Lambda_\Gamma}(0)} \|\lambda_1 - \bar{\lambda}\|^2$$

when  $R_1 - R_2 = C$  for some constant  $C$ .

*Proof:* For our sequence of lattices

$$\begin{aligned} 0 & \leq \lim_{R_1 \rightarrow \infty} \frac{\sum_{\lambda \in V_{\Lambda_\Gamma}(0)} \|\lambda_1 - \bar{\lambda}\| \|\bar{\lambda} - \lambda\|}{\sum_{\lambda \in V_{\Lambda_\Gamma}(0)} \|\lambda_1 - \bar{\lambda}\|^2} \\ & \leq \lim_{R_1 \rightarrow \infty} \rho_\Gamma \frac{\sum_{\lambda \in V_{\Lambda_\Gamma}(0)} \|\lambda_1 - \bar{\lambda}\|}{\sum_{\lambda \in V_{\Lambda_\Gamma}(0)} \|\lambda_1 - \bar{\lambda}\|^2} \\ & = \lim_{R_1 \rightarrow \infty} \rho_\Gamma \frac{\sum_{\lambda \in V_{\Lambda_\Gamma}(0)} \frac{\gamma_2}{\gamma_1 + \gamma_2} \|\lambda_1 - \lambda_2\|}{\sum_{\lambda \in V_{\Lambda_\Gamma}(0)} \left( \frac{\gamma_2}{\gamma_1 + \gamma_2} \right)^2 \|\lambda_1 - \lambda_2\|^2} \\ & = \lim_{R_1 \rightarrow \infty} \rho_\Gamma \left( \frac{\gamma_1 + \gamma_2}{\gamma_2} \right) \frac{\sum_{\lambda \in V_{\Lambda_\Gamma}(0)} \|\lambda_1 - \lambda_2\|}{\sum_{\lambda \in V_{\Lambda_\Gamma}(0)} \|\lambda_1 - \lambda_2\|^2} \\ & = \lim_{R_1 \rightarrow \infty} \rho_\Gamma \left( \frac{\gamma_1 + \gamma_2}{\gamma_2} \right) \frac{\sum_{\lambda_1 \in V_{\Lambda_\Gamma}(0)} \sum_{\lambda_2 \in V_{\Lambda_s}(\lambda_1)} \|\lambda_1 - \lambda_2\|}{\sum_{\lambda_1 \in V_{\Lambda_\Gamma}(0)} \sum_{\lambda_2 \in V_{\Lambda_s}(\lambda_1)} \|\lambda_1 - \lambda_2\|^2} \end{aligned}$$

$$\leq \lim_{R_1 \rightarrow \infty} P \left( \frac{\gamma_1 + \gamma_2}{\gamma_2} \right) \frac{\rho_\Gamma}{\nu_s^{1/L}} \quad (73)$$

where  $P = \frac{G_1(\bar{\Lambda}_s)}{G(\bar{\Lambda}_s)}$  is a dimensionless constant that depends on  $\bar{\Lambda}_s$ , with  $G(\bar{\Lambda}_s)$  the normalized second moment and

$$G_1(\bar{\Lambda}_s) = \frac{\int_{V_s(\lambda_1)} \|x - \lambda_1\| dx}{\nu_s^{(1+1/L)}}$$

is the normalized absolute first moment. Therefore,  $P$  is scale-invariant and dimensionless. Now the scaling  $\beta$  affects  $\nu_s$  by changing it to  $\nu_s \beta^L$ . Also, the scaling affects  $\rho_\Gamma$  by scaling it to  $\beta \rho_\Gamma$ . As

$$\frac{\rho_\Gamma}{\nu_s^{1/L}} = \frac{\Theta(\beta n)}{\Theta(\beta n^2)} = \Theta(n^{-1})$$

we obtain

$$\lim_{R_1 \rightarrow \infty} \frac{\rho_\Gamma}{\nu_s^{1/L}} = \lim_{n \rightarrow \infty} \frac{\rho_\Gamma}{\nu_s^{1/L}} = 0$$

so the expression in (73) goes to zero asymptotically in the rate.

In a similar manner we can show that

$$\begin{aligned} 0 & \leq \lim_{R_1 \rightarrow \infty} \frac{\sum_{\lambda \in V_{\Lambda_\Gamma}(0)} \|\bar{\lambda} - \lambda\|^2}{\sum_{\lambda \in V_{\Lambda_\Gamma}(0)} \|\lambda_1 - \bar{\lambda}\|^2} \\ & \leq \lim_{R_1 \rightarrow \infty} \rho_\Gamma^2 \frac{N_\Gamma}{\sum_{\lambda \in V_{\Lambda_\Gamma}(0)} \|\lambda_1 - \bar{\lambda}\|^2} \\ & \leq G(\Lambda_s) \frac{\gamma_2^2}{(\gamma_1 + \gamma_2)^2} \lim_{R_1 \rightarrow \infty} \left[ \frac{\rho_\Gamma}{\nu_s^{1/L}} \right]^2 = 0. \end{aligned} \quad (74)$$

Using these in (72) we obtain the desired result.  $\square$

Using Lemma V.1, we can write

$$\begin{aligned} \sum_{\lambda \in V_{\Lambda_\Gamma}(0)} \|\lambda - \lambda_1\|^2 & \approx \sum_{\lambda \in V_{\Lambda_\Gamma}(0)} \|\lambda_1 - \bar{\lambda}\|^2 \\ & = \frac{\gamma_2^2}{(\gamma_1 + \gamma_2)^2} \sum_{\lambda \in V_{\Lambda_\Gamma}(0)} \|\lambda_1 - \lambda_2\|^2 \end{aligned} \quad (75)$$

for sufficiently high rates. Therefore, the side distortions are directly related to  $J_s$  which was calculated earlier. Hence, the side distortions are approximated by

$$\begin{aligned} \bar{d}_1 & \approx \frac{\gamma_2^2}{(\gamma_1 + \gamma_2)^2} G(\Lambda_s) 2^{2h(p)} 2^{-2(R_1 + R_2 - R_0)} \\ \bar{d}_2 & \approx \frac{\gamma_1^2}{(\gamma_1 + \gamma_2)^2} G(\Lambda_s) 2^{2h(p)} 2^{-2(R_1 + R_2 - R_0)}. \end{aligned} \quad (76)$$

It follows that the distortion ratio  $\frac{\bar{d}_1}{\bar{d}_2}$  is approximately  $\left(\frac{\gamma_2}{\gamma_1}\right)^2$ , a convenient formula when designing the lattice quantizer. Although this is only a high-rate approximation, the examples have shown that it is also a useful formula at lower rates.

Next we examine the case when  $\gamma_1 \neq 0$ ,  $\gamma_2 = 0$ . In this case, we can show that

$$\begin{aligned} \bar{d}_1 & \approx G(\Lambda_s) 2^{2h(p)} 2^{-2R_1} \\ \bar{d}_2 & \approx G(\Lambda_s) 2^{2h(p)} 2^{-2(R_1 + R_2 - R_0)}. \end{aligned} \quad (77)$$

The roles are reversed when  $\gamma_1 = 0$  and  $\gamma_2 \neq 0$ . It is worth noting that in a successive refinement scheme [10], the expression for  $\bar{d}_2$  (for  $\gamma_1 \neq 0$ ,  $\gamma_2 = 0$ ) does not decay exponentially

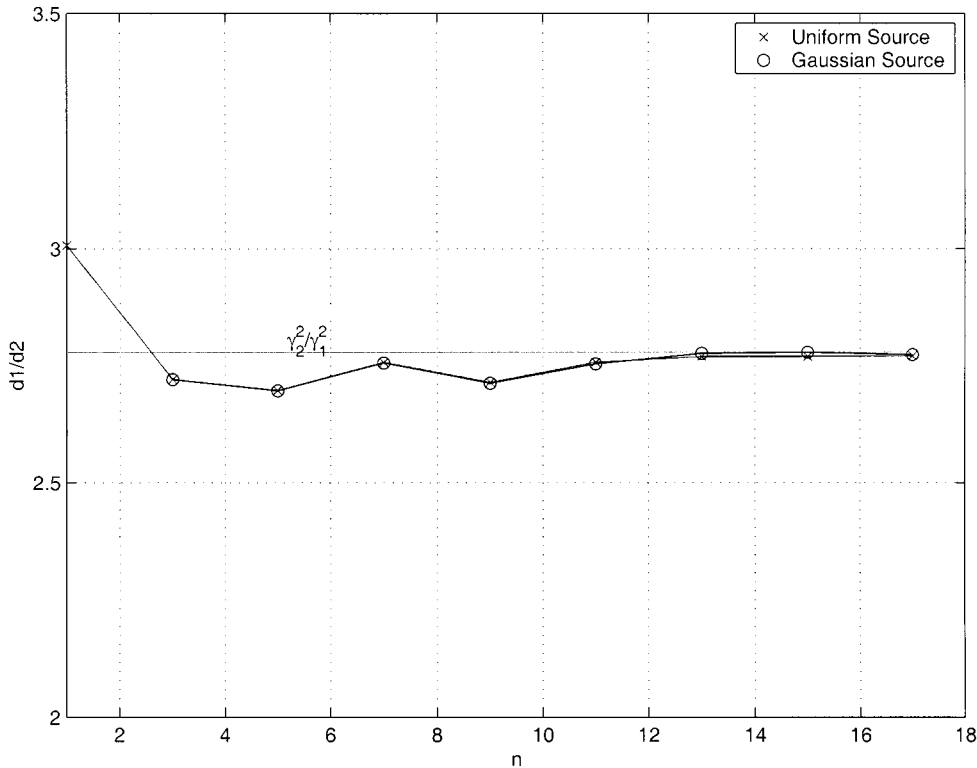


Fig. 11. Comparison of side distortion ratio to  $\frac{\gamma_2^2}{\gamma_1^2}$  predicted by the rate asymptotics in (76).

with rate, since the diameter of the set  $\{\lambda: \alpha_2(\lambda) = \lambda_2'\}$  is bounded away from zero.

Let  $R_0 = \frac{R_1 + R_2}{2} (1 + a)$ , so that

$$R_1 + R_2 - R_0 = \frac{R_1 + R_2}{2} (1 - a).$$

Note that  $a$  is chosen so that  $a > \frac{|R_1 - R_2|}{R_1 + R_2}$  and, therefore,  $R_1 + R_2 - R_0 < \min(R_1, R_2)$ . Here we can clearly see the tradeoff between the central distortion  $\bar{d}_0$  and the side distortions.

### B. Minimizing Average Distortion

Suppose we know that the packet loss probability on channel 1 is  $p_1$  and the packet loss probability on channel 2 is  $p_2$ . Then the average distortion is given by

$$\bar{D} = (1 - p_1)(1 - p_2)\bar{d}_0 + (1 - p_1)p_2\bar{d}_1 + (1 - p_2)p_1\bar{d}_2 + p_1p_2E[||\mathbf{x}'||^2]. \quad (78)$$

Using the high-rate approximations developed earlier, we can find the optimal  $\frac{\gamma_1}{\gamma_2}$  needed for minimizing the distortion.

*Claim V.1:* The weights which minimize (78) at high rate are given by

$$\frac{\gamma_1}{\gamma_2} = \frac{(1 - p_1)p_2}{(1 - p_2)p_1}. \quad (79)$$

*Proof:* To optimize (78) we use the high-rate expressions given in (76). Using (76) in (78) we obtain

$$\bar{D} = A + B_1 \left( \frac{\gamma_1}{\gamma_1 + \gamma_2} \right)^2 + B_2 \left( \frac{\gamma_2}{\gamma_1 + \gamma_2} \right)^2 \quad (80)$$

where  $A, B_1, B_2$  do not depend on  $\gamma_1, \gamma_2$  (they depend on  $R_1, R_2, R_0, \beta, p_1, p_2$ ). Without loss of generality, we can use  $\bar{\gamma}_1 = \frac{\gamma_1}{\gamma_1 + \gamma_2}$  and  $\bar{\gamma}_2 = \frac{\gamma_2}{\gamma_1 + \gamma_2}$ . Hence, defining  $\gamma = \bar{\gamma}_1 = 1 - \bar{\gamma}_2$  and substituting in (80) we obtain

$$\bar{D} = A + B_1\gamma^2 + B_2(1 - \gamma)^2. \quad (81)$$

By differentiating (81) with respect to  $\gamma$  and setting it to zero we obtain the given result. Note that this problem is convex (the second derivative of (81) is positive) and hence we have obtained the minimum<sup>6</sup> with respect to  $\gamma$ .  $\square$

## VI. NUMERICAL RESULTS

In this section, we illustrate the performance of the proposed quantizer and compare it to both information-theoretic bounds and also the high-rate asymptotic analysis developed in Section V. In comparisons of its performance with that predicted by information theory, we assume that there is an entropy (lossless) coding of the quantizer output. For a Gaussian source, the multiple description rate-distortion problem was solved by Ozarow [22], El Gamal and Cover [9].

In the first example, we design a scalar quantizer and compare its performance to the high-rate asymptotic results presented in Section V. We start with a base lattice  $\Lambda = \mathbb{Z}$  and use  $N_1 = 5, N_2 = 3$  with  $N_1(n) = 5n, N_2(n) = 3n$  for

<sup>6</sup>A referee pointed out an alternative way to see this result. Note that in (78) only the first three terms depend on  $\gamma_1, \gamma_2$  and so without that term the equation is identical in form to (11) with the substitution  $\gamma_1 \leftrightarrow (1 - p_1)p_2, \gamma_2 \leftrightarrow (1 - p_2)p_1$ . Therefore,  $\bar{D}$  is minimized by taking  $\gamma_1 = (1 - p_1)p_2, \gamma_2 = (1 - p_2)p_1$ .

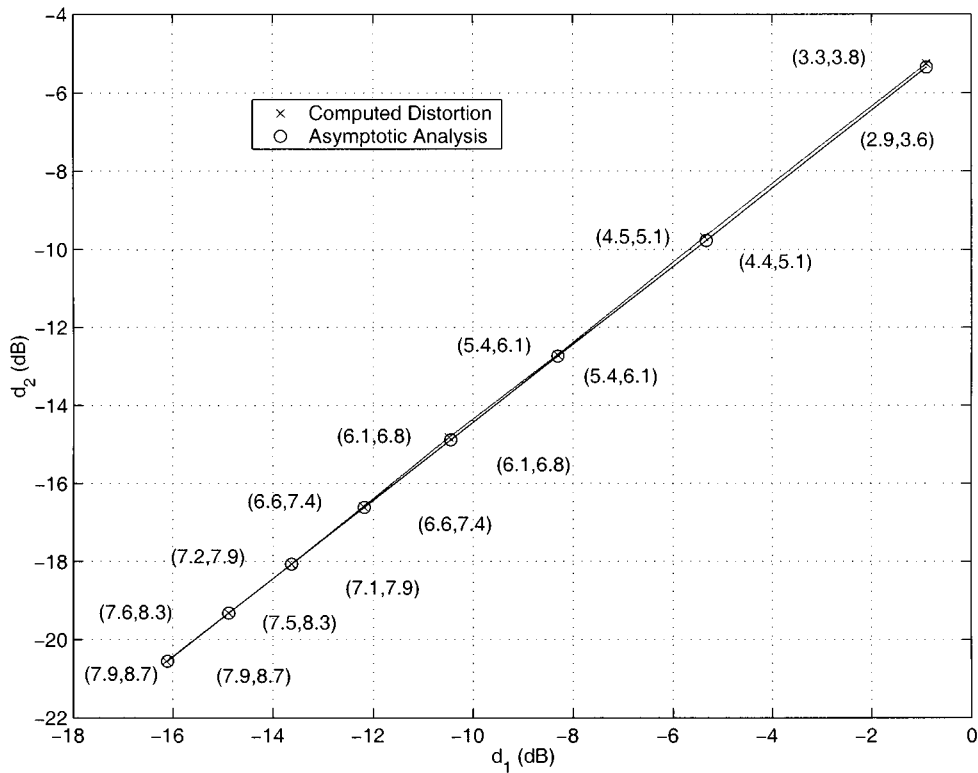


Fig. 12. Comparison of side distortions and rates with the high-rate asymptotics predictions in (76) and (59).

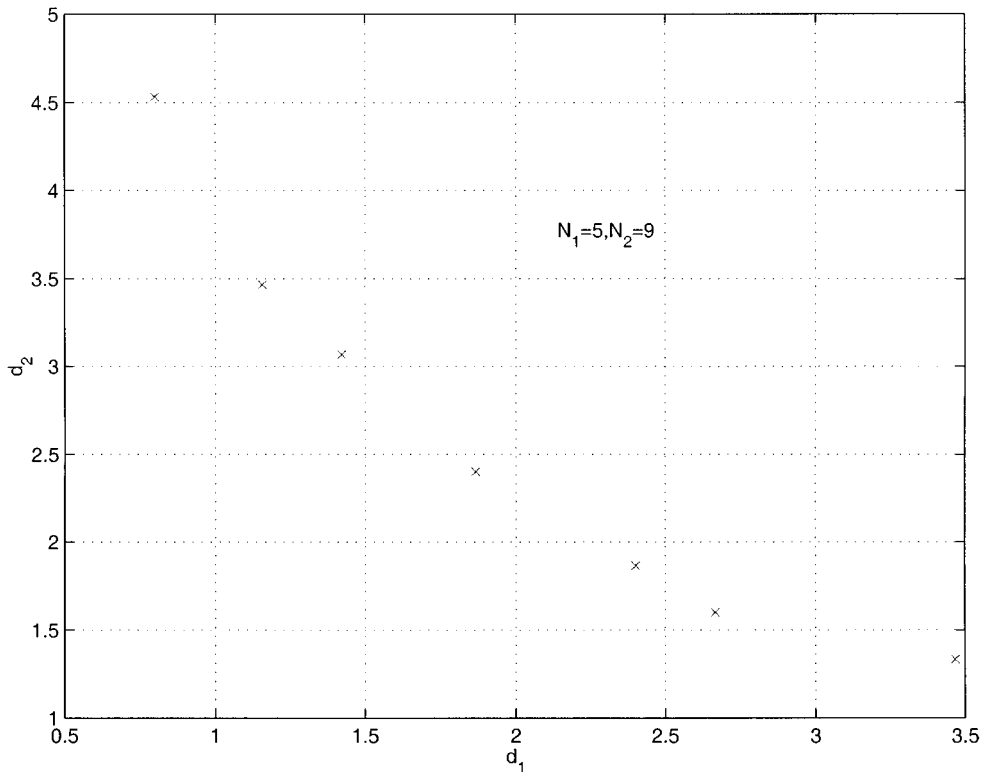


Fig. 13. Side distortions for fixed sublattices with varying  $\gamma_1, \gamma_2$ .

the asymptotic growth. We use a step size of  $\beta = \frac{1}{n^3}$  to ensure that the rate scaling takes place. In Fig. 11 we illustrate the rapid convergence of the distortion ratio  $\bar{d}_1/\bar{d}_2$  to the asymptotic value  $\gamma_2^2/\gamma_1^2$  as predicted in (76). This is shown for both Gaussian and uniform sources.

Next, in Fig. 12, we compare the distortion and the rates of the quantizer to that predicted by the high rate asymptotics in (76) and (59). Each numerically obtained distortion pair is tagged with two rate pairs. The rates predicted by (59) are below the  $(\bar{d}_1, \bar{d}_2)$  curve and the rates of the quantizer (numerically ob-

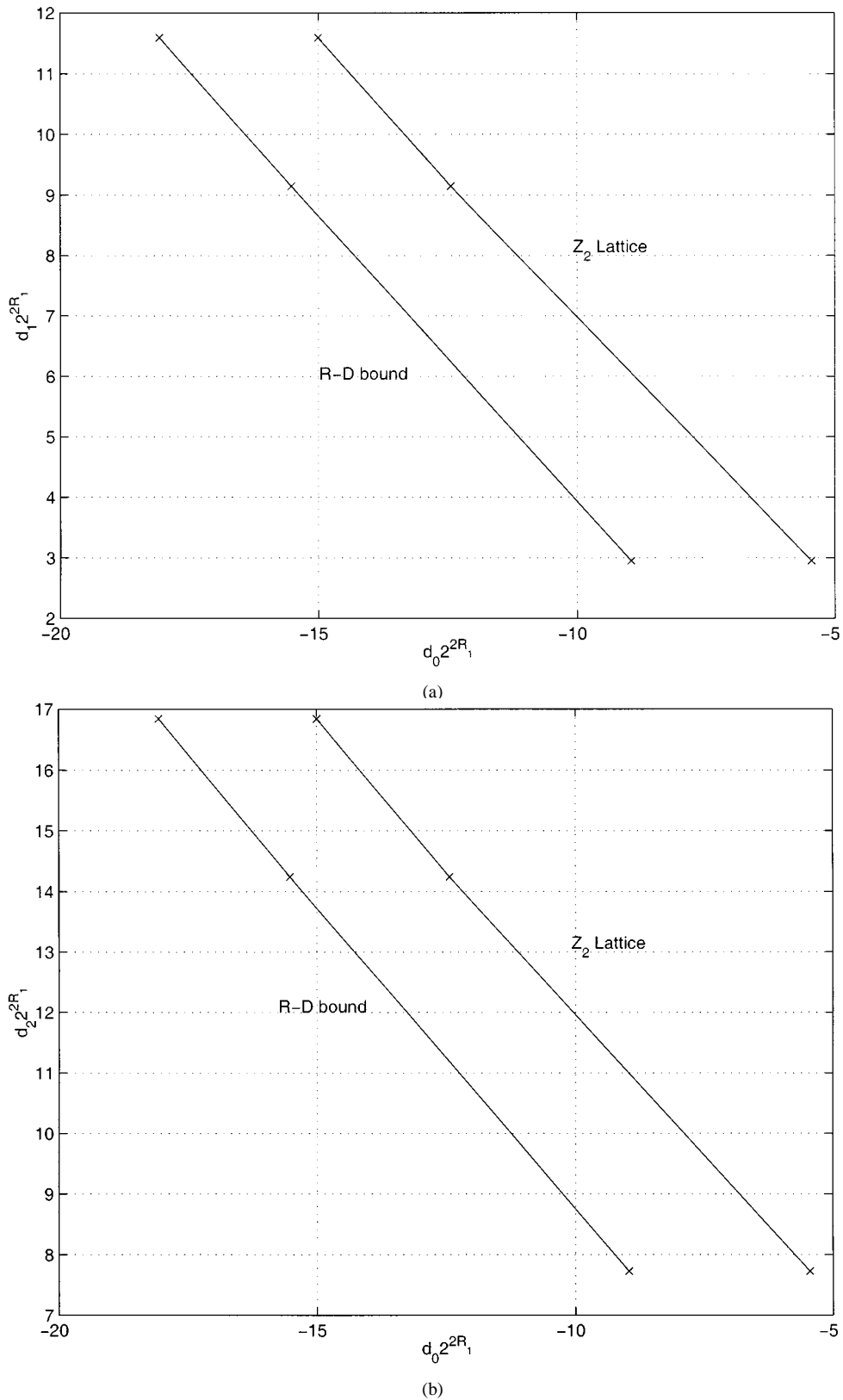


Fig. 14. Comparison of lattice distortion with rate-distortion bound.

tained) are above the curve. This is done for a unit variance Gaussian source. As can be seen from the figure, the high-rate predictions are quite accurate.

The vector quantizer is illustrated with the  $\mathbb{Z}^2$  lattice that we described in Section III. The rates are chosen so that

$R_1 - R_2 = \frac{1}{2} \log_2 \left( \frac{|\Lambda_2|}{|\Lambda_1|} \right)$ . In Fig. 13 we illustrate the tradeoff between the two side distortions by varying  $\gamma_1, \gamma_2$ . In Fig. 14 we have plotted the side distortions and compared them with those predicted by information theory [22]. The key observation is that the distortion performance of the lattice

quantizer is approximately 3 dB away from that predicted by the rate-distortion bound. This gap is due to the shaping gain that we will pick up when we go to higher dimensions and using sublattices which have Voronoi cells which are closer to spherical. The  $\mathbb{Z}^2$  lattice used in this example is more for illustrative purposes and has very little shaping gain.

## VII. DISCUSSION

In this paper, we have designed asymmetric multiple description lattice quantizers. This source coding scheme bridges the symmetric (balanced) multiple description quantizers and completely hierarchical successive refinement quantizers. Though a lattice vector quantizer was illustrated, this scheme could also be extended to other types of source coding schemes.

## ACKNOWLEDGMENT

The authors greatly appreciate the careful reading and insightful comments on the paper by the referees.

## REFERENCES

- [1] R. Balan, I. Daubechies, and V. A. Vaishampayan, "Trading rate for distortion through varying the redundancy of a windowed Fourier frame in a multiple description compression," preprint, 1999.
- [2] P. A. Chou, S. Mehrotra, and A. Wang, "Decoding of overcomplete expansions using projections onto convex sets," in *Proc. Data Compression Conf.*, Mar. 29–31, 1999, pp. 72–81.
- [3] J. H. Conway, E. M. Rains, and N. J. A. Sloane, "On the existence of similar sublattices," *Canad. J. Math.*, vol. 51, pp. 1300–1306, 1999.
- [4] J. H. Conway and N. J. A. Sloane, "The cell structures of certain lattices," in *Miscellanea Mathematica*, P. Hilton, F. Hirzebruch, and R. Remmert, Eds. New York: Springer-Verlag, 1991, pp. 71–107.
- [5] —, *Sphere Packings, Lattices and Groups*, 3rd ed. New York: Springer-Verlag, 1998.
- [6] D. Cox, *Primes of the Form  $x^2 + ny^2$* . New York: Wiley, 1989.
- [7] "CPLEX Manual," CPLEX Organization Inc., Incline Village, NV, 1991.
- [8] L. E. Dickson, *Algebras and Their Arithmetics*. New York: Dover, 1960.
- [9] A. A. El Gamal and T. M. Cover, "Achievable rates for multiple descriptions," *IEEE Trans. Inform. Theory*, vol. IT-28, pp. 851–857, Nov. 1982.
- [10] W. H. R. Equitz and T. M. Cover, "Successive refinement of information," *IEEE Trans. Inform. Theory*, vol. 37, pp. 269–275, Mar. 1991.
- [11] M. Fleming and M. Effros, "Generalized multiple description vector quantization," in *Proc. Data Compression Conf.*, Mar. 29–31, 1999, pp. 3–12.
- [12] R. Fourer, D. M. Gay, and B. W. Kernighan, *AMPL: A Modeling Language for Mathematical Programming*. San Francisco, CA: Scientific, 1993.
- [13] V. K. Goyal, J. Kovacevic, and M. Vetterli, "Quantized frame expansions as source-channel codes for erasure channels," in *Proc. Data Compression Conf.*, Mar. 29–31, 1999, pp. 326–335.
- [14] R. M. Gray, *Source Coding Theory*. Norwell, MA: Kluwer, 1990.
- [15] G. H. Hardy and E. M. Wright, *An Introduction to the Theory of Numbers*, 5th ed. U.K.: Oxford Univ. Press, 1980.
- [16] A. Ingle and V. A. Vaishampayan, "DPCM system design for diversity systems with applications to packetized speech," *IEEE Trans. Speech Audio Processing*, vol. 1, pp. 48–58, Jan. 1995.
- [17] H. Jafarkhani and V. Tarokh, "Multiple description trellis coded quantizers," *IEEE Trans. Commun.*, vol. 47, pp. 799–803, June 1999.
- [18] D. G. Luenberger, *Linear and Non-Linear Programming*, 2nd ed. Reading, MA: Addison-Wesley, 1984.
- [19] A. E. Mohr, E. A. Riskin, and R. E. Ladner, "Graceful degradation over packet erasure channels through forward error correction," in *Proc. Data Compression Conf.*, Mar. 29–31, 1999, pp. 92–101.
- [20] G. Nebe and N. J. A. Sloane. (2001) *A Catalogue of Lattices*. [Online]. Available: [www.research.att.com/~njas/lattices/](http://www.research.att.com/~njas/lattices/).
- [21] M. Orchard, Y. Wang, V. A. Vaishampayan, and A. Reibman, "Redundancy rate distortion analysis of multiple description coding using pairwise correlating transforms," in *Proc. 1997 Int. Conf. Image Processing*, Oct. 1997.
- [22] L. Ozarow, "On a source coding problem with two channels and three receivers," *Bell Syst. Tech. J.*, vol. 59, pp. 1909–1921, Dec. 1980.
- [23] J. J. Rotman, *An Introduction to the Theory of Groups*, 4th ed. New York: Springer-Verlag, 1995.
- [24] N. J. A. Sloane. *The On-Line Encyclopedia of Integer Sequences*. [Online]. Available: [www.research.att.com/~njas/sequences](http://www.research.att.com/~njas/sequences).
- [25] V. A. Vaishampayan, "Vector quantizer design for diversity systems," in *Proc. 25th Annu. Conf. Information Sciences and Systems*, Johns Hopkins Univ., Baltimore, MD, Mar. 20–22, 1991, pp. 564–569.
- [26] —, "Design of multiple description scalar quantizers," *IEEE Trans. Inform. Theory*, vol. 39, pp. 821–834, May 1993.
- [27] V. A. Vaishampayan and A. A. Siddiqui, "Speech predictor design for diversity communication systems," in *Proc. 1995 IEEE Speech Coding Workshop*, Sept. 20–22, 1995.
- [28] V. A. Vaishampayan, N. J. A. Sloane, and S. D. Servetto, "Multiple-description vector quantization with lattice codebooks: Design and analysis," *IEEE Trans. Inform. Theory*, vol. 47, pp. 1718–1734, July 2001.
- [29] J. K. Wolf, A. D. Wyner, and J. Ziv, "Source coding for multiple descriptions," *Bell Syst. Tech. J.*, vol. 59, pp. 1417–1426, Oct. 1980.
- [30] Z. Zhang and T. Berger, "New results in binary multiple descriptions," *IEEE Trans. Inform. Theory*, vol. IT-33, pp. 502–521, July 1987.